研究成果の刊行に関する一覧表（平成20～22年度）

発表者氏名	論文タイトル名	発表誌名	巻号	ページ	出版年
Cushing, B.S., Perry, A., Musatov, S., Ogawa, S. and Papademetriou E.	Estrogen receptors in the medial amygdala inhibit the expression of male prosocial behavior.	Journal of Neuroscience	28	10399-10403	2008
Mitsushima D, Takase K, Funabashi T, Kimura F.	Gonadal steroid hormones maintain the stress-induced acetylcholine release in the hippocampus: simultaneous measurements of the extracellular acetylcholine and serum corticosterone levels in the same subjects.	Endocrinology	149	802-811	2008
Tsukahara S, Hojo R, Kuroda Y, Fujimaki H.	Estrogen modulates Bcl-2 family protein expression in the sexually dimorphic nucleus of the preoptic area of postnatal rats.	Neurosci Lett.	432	58-63	2008
Kawashima T, Okuno H, Nonaka M, Adachi-Morishima A, Kyo N, Okamura M, Takemoto-Kimura S, Worley PF, Bito H.	A synaptic activity-responsive element in the Arc/Arg3.1 promoter essential for synapse-to-nucleus signaling in activated neurons.	Proc. Natl. Acad. Sci. USA USA	106	316-321	2009
Crews, D., Rushworth, D., Gonzalez-Lima, F. and Ogawa, S.	Litter environment affects behavior and brain metabolic activity of adult knockout mice.	Frontiers in Behavioral Neuroscience	3	Article 12	2009

発表者氏名	論文タイトル名	発表誌名	巻号	ページ	出版年
Hagiwara H, Ishida M, Arita J, Mitsushima D, Takahashi T, Kimura F, Funabashi T.	The cAMP response element-binding protein in the bed nucleus of the stria terminalis modulates the formalin-induced pain behavior in the female rat.	Eur J Neurosci.	30(12)	2379-2386	2009
Tomihara, K., Soga, T., Nomura, M., Korach, K.S., Gustafsson, J-Å, Pfaff, D.W., and Ogawa, S.	Effect of ER-β gene disruption on estrogenic regulation of anxiety in female mice.	Physiology and Behavior	96	300-306	2009
Mitsushima D, Takase K, Funabashi T, Kimura F.	Gonadal steroids maintain 24 h acetylcholine release in the hippocampus: organizational and activational effects in behaving rats.	J Neurosci.	29	3808-3815	2009
Tsukahara S, Nakajima D, Kuroda Y, Hojo R, Kageyama S, Fujimaki H.	Effects of maternal toluene exposure on testosterone levels in fetal rats.	Toxicol Lett.	185	79-84	2009
Haijima A, Endo T, Zhang Y, Miyazaki W, Kakeyama M (Corresponding Author), Tohyama C.	In utero and lactational exposure to low doses of chlorinated and brominated dioxins induces deficits in the fear memory of male mice.	Neurotoxicology	31	385-390	2010

発表者氏名	論文タイトル名	発表誌名	巻号	ページ	出版年
Nakamura, N.H., Fukunaga, M., Akama, K.T., Soga, T., Ogawa, S., and Pavlides, C.	Hippocampal cells encode places by forming small anatomical clusters.	Neuroscience	166	994-1007	2010
Spiteri, T., Musatov, S., Ogawa, S., Ribeiro, A., Pfaff, D.W., and Agmo, A.	The role of the estrogen receptor alpha in the medial amygdala and ventromedial nucleus of the hypothalamus in social recognition, anxiety and aggression.	Behavioural Brain Research	210	211-220	2010
Lei, K., Cusing, B.S., Musatov, S., Ogawa, S., and Kramer, K.M.	Estrogen receptor-alpha in the bed nucleus of the stria terminalis regulates social affiliation in male prairie voles (Microtus ochrogaster).	PLoS One	5	e8931	2010
Furuta M, Mitsushima D, Shinohara K, Kimura F, Funabashi T.	Food availability affects orexin a/ hypocretin-1-induced inhibition of pulsatile luteinizing hormone secretion in female rats.	Neuroendocrinology	91	41-47	2010
Funabashi T, Furuta M, Fukushima A, Kimura F.	Age- and sex-specific changes in naloxone-induced luteinizing hormone secretion and Fos expression in gonadotropin-releasing hormone neurons of gonadectomized rats.	Neurosci Lett.	471	157-161	2010

発表者氏名	論文タイトル名	発表誌名		ページ	出版
Hagiwara H, Kimura F, Mitsushima D, Funabashi T.	Formalin-induced nociceptive behavior and c-Fos expression in middle-aged female rats.	Physiol Behav.	100	101-104	2010
Bito, H.	The chemical biology of synapses and neuronal circuits.	Nature Chem.Biol.	6	560-563	2010
Win-Shwe TT, Tsukahara S, Yamamoto S, Fukushima A, Kunugita N, Arashidani K,	Up-regulation of neurotrophin-related gene expression in mouse hippocampus following low-level toluene exposure.	Neurotoxicology	31	85-93	2010
Koike-Kuroda Y, Kakeyama M, Fujimaki H,Tsukahara S.	Use of live imaging analysis for evaluation of cytotoxic chemicals that induce apoptotic cell death.	Toxicol In Vitro.	24	2012-2020	2010
Tsukahara S, Tsuda MC., Kurihara R, Kato Y, Kuroda Y, Nakata M, Xiao K, Nagata K, Toda K, Ogawa S.	Effects of aromatase or estrogen receptor gene deletion on masculinization of the principal nucleus of the bed nucleus of the stria terminalis of mice.	Neuroendocrinology	2011 Apr 22		Epub ahead of print
Tsuda MC, Yamaguchi N, Ogawa S.	Early life stress disrupts peri-pubertal development of aggression in male mice.	Neuroreport	22	259-263	2011

発表者氏名	論文タイトル名	発表誌名		ページ	出版
Endo T, Maekawa F, Võikar V, Haijima A, Uemura Y, Zhang Y, Miyazaki W, Suyama S, Shimazaki K, Wolfer DP, Yada T, Tohyama C, Lipp HP, Kakeyama M.	Automated test of behavioral flexibility in mice using a behavioral sequencing task in IntelliCage.	Behav Brain Res.	221(1)	172-81	2011

研究成果の刊行物・別刷

＊現在の資源・エネルギー事情を踏まえて、本研究課題の集大成というべき一報(Endo *et al.* 2011、本冊子の末尾に掲載)を除いて、別刷は2ページを1項に縮小、モノクロ印刷とさせていただきました。

Behavioral/Systems/Cognitive

Estrogen Receptors in the Medial Amygdala Inhibit the Expression of Male Prosocial Behavior

Bruce S. Cushing,[1,2,3] Adam Perry,[3] Sergei Musatov,[4,5] Sonoko Ogawa,[6] and Eros Papademetriou[3]

[1]Department of Biology and [2]Integrated Bioscience Program, The University of Akron, Akron, Ohio 44325-3908, [3]The Brain–Body Center, Department of Psychiatry, University of Illinois at Chicago, Chicago, Illinois 60612, [4]Neurologix, Fort Lee, New Jersey 07024, [5]Laboratory of Neurobiology and Behavior, The Rockefeller University, New York, New York 10021, and [6]Kansei Behavioral and Brain Sciences Graduate School of Comprehensive Human Sciences, University of Tsukuba, Tsukuba, Ibaraki 305-8577, Japan

Studies using estrogen receptor α (ERα) knock-out mice indicate that ERα masculinizes male behavior. Recent studies of ERα and male prosocial behavior have shown an inverse relationship between ERα expression in regions of the brain that regulate social behavior, including the medial amygdala (MeA), and the expression of male prosocial behavior. These studies have lead to the hypothesis that low levels of ERα are necessary to "permit" the expression of high levels of male prosocial behavior. To test this, viral vectors were used to enhance ERα in male prairie voles (*Microtus ochrogaster*), which display high levels of prosocial behavior and low levels of MeA ERα. Adult male prairie voles were transfected with ERα in the MeA (MeA-ERα) or the caudate–putamen (ERα control) or luciferase (MeA-site-specific control), and 3 weeks later tested for spontaneous alloparental behavior and partner preference. Enhancing ERα in the MeA altered/reduced male prosocial behavior. Only one-third of MeA-ERα males, compared with all control males, were alloparental. MeA-ERα males also displayed a significant preference for a novel female. This is a critical finding because the manipulations of neuropeptides, oxytocin and vasopressin, can inhibit the formation of a partner preference, but do not lead to the formation of a preference for a novel female. The results support the hypothesis that low levels of ERα are necessary for high levels of male prosocial behavior, and provide the first direct evidence that site-specific ERα expression plays a critical role in the expression of male prosocial behavior.

Key words: estrogen receptor α; *Microtus ochrogaster*; transfection; viral vector; aggression; amygdala

Introduction

Estrogen plays a critical role in the expression of male social behavior. Studies using estrogen receptor (ER) knock-out mice indicate that ERα and ERβ regulate different aspects of male behavior. ERβ is involved in defeminization (Kudwa et al., 2005), anxiety, and cognition (Krezel et al., 2001), whereas ERα masculinizes behavior (Ogawa et al., 1998; Wersinger et al., 1997). Although some males display high levels of prosocial behavior and positive affiliative behavior, masculine behavior is typically associated with low levels of prosocial behavior and high levels of aggression. The expression of high levels of prosocial behavior requires a reduction of "typical" masculine behavior. It has been hypothesized that decreasing ERα within the social neural circuit is "necessary" for the expression of high levels of prosocial behavior (Cushing et al., 2004; Cushing and Wynne-Edwards, 2006).

Comparative studies support this hypothesis. Illinois prairie voles (*Microtus ochrogaster*) are highly social, forming pair bonds and providing biparental care. However, Kansas males are significantly less social (Cushing and Kramer, 2005a) and express significantly higher levels of ERα in the medial amygdala (MeA) and bed nucleus of the stria terminals (BST) than Illinois males (Cushing et al., 2004). Socially monogamous pine voles (*M. pinetorum*) express lower levels of ERα than the polygynous meadow (*M. pennsylvanicus*) and montane voles (*M. montanus*) (Cushing and Wynne-Edwards, 2006). Finally, male ERα in species of two dwarf hamsters (*Phodopus* sp.) that differ in social behavior mirrored ERα expression within prairie vole populations (Cushing and Wynne-Edwards, 2006).

Changes in ERα expression are correlated with prosocial behavior. In male prairie voles, neonatal castration eliminated alloparental behavior (Lonstein et al., 2002) and the ability of neuropeptides to stimulate pair bond formation (Cushing et al., 2003), whereas significantly increasing ERα in specific brain regions, including the MeA (Cushing and Kramer, 2005b). Long-day male Siberian hamsters (*Phodopus sungorus*) are nonaggressive, although aggression increases under short days, which is associated with increased ERα (Kramer et al., 2008). Finally, in mice male aggression has been associated with individual variation in ERα (Trainor et al., 2006). These findings are significant, but correlative. Therefore our goal was to increase ERα in the MeA of male prairie voles and test the prediction that this would disrupt prosocial behavior.

This study focused on the MeA. MeA ERα is inversely correlated with male prosocial behavior (Hnatczuk et al., 1994; Cushing et al., 2004; Cushing and Wynne-Edwards, 2006). Conspecific odors activate the vomeronasal organ, triggering the MeA and BST, leading to stimulation of the rest of the social neural circuit (Newman, 1999). Additionally, the MeA innervates the "reward" system via the ventral pallidum, and the reward system is critical for long-term social bond formation (Young et al., 2005). Finally, the MeA regulates social recognition/memory (Ferguson et al., 2001), which is a necessary for long-term social bond formation. We are not suggesting that the MeA is the primarily responsible for regulating specific social behaviors, but that it is critical for the initiation of social responses and therefore changes in MeA can and will impact many aspects of the social response.

Received May 2, 2008; revised Aug. 24, 2008; accepted Aug. 24, 2008.

This work was supported by National Institute of Mental Health Grants MH068278 and MH001992 (B.S.C.). We thank K. Kramer and N. Cushing for their comments and suggestions on this manuscript and K. Sharer for stereotaxic advice.

Correspondence should be addressed to Bruce S. Cushing, Department of Biology and Integrated Bioscience Program, The University of Akron, Akron, OH 44325-3908. E-mail: cbruce@uakron.edu.

DOI:10.1523/JNEUROSCI.1928-08.2008

 0270-6474/08/2810399-05$15.00/0

Materials and Methods

Animal husbandry

Animals used in this study were laboratory-reared prairie voles that originated from wild stock trapped near Urbana, IL. Animals were housed under a 14 h/10 h light/dark cycle and provided high fiber rabbit chow and water *ad libitum*. Animals were housed in accordance with the United States Department of Agriculture and National Institutes of Health guidelines and all procedures were approved by the University of Illinois at Chicago Animal Care and Use Committee before undertaking any experimental manipulation.

Viral vector transfection

To achieve site-specific overexpression of ERα in the MeA, adult males (60–70 d of age) were stereotactically injected, bilaterally, with adenoassociated viral (AAV) vectors encoding human ERα. The site of the MeA was determined to be −1.25 mm anteroposterior, ±1.65 mm mediolateral, and −5.8 mm dorsal from bregma. Two controls were established. Site-specific controls were generated by transfecting the MeA of males with a similar vector encoding firefly luciferase cDNA, and ERα controls were generated by transfecting the caudate–putamen with ERα. Caudate neurons do not express ERα. The AAV vectors used in this study have been described previously in detail (Musatov et al., 2006). Briefly, the vectors express short hairpin RNA containing ERα (GGCATGGAGCATCTCTACA) or luciferase (CCGCTGGAGAGCAACTGCAT) target sequences under the control of the human H1 promoter. In addition, both vectors were designed to express enhanced green fluorescent protein (GFP) as a reporter to visualize transfection neurons and placed under a control of a hybrid cytomegalovirus/chicken-β-actin promoter to ensure stable long-term expression. Vector stocks were generated using a helper-free AAV-2 plasmid transfection system, purified by heparin affinity chromatography and dialyzed against PBS as described previously (Clark et al., 1999). AAV genomic titers were determined by quantitative PCR and adjusted to 109 particles per microliter. Three weeks after transfection males began behavioral testing. After completion of behavioral testing, males were killed to analyze the efficiency of gene transfer, and behavioral data were only analyzed in males in which transfection was verified.

Verification of transfection. After completion of the social preference test, brains from experimental animals were fixed using transcardial perfusion, sectioned at 30 μm on a freezing sliding microtome, and then the free-floating sections were stained for ERα using standard AB immunocytochemistry (for complete details, see Cushing et al., 2004). The human-specific primary antibody RM9101-s (Neomarkers; 1:1000 dilution) was used to label transfected ERα and then visualized using DAB. RM9101-s does not label prairie vole ERα. Therefore, all ERα observed with this antibody were the product of transfection. Successful transfection was determined qualitatively by visually examining ERα expression using a Nikon E-800 microscope. It should be noted that there were no animals that display only a few transfected ERα-immunoreactive cells, and transfected males either displayed no or a significant amount of transfected ERα. Figure 1*a* shows a typical level of transfected ERα expression, which is compared with nontransfected ERα expression seen in Figure 1*b*. Only animals that showed at least unilateral ERα expression resulting from transfection in the MeA, were used in subsequent analysis of behavior data. Luciferase expression was determined by examining tissue for GFP expression (see Fig. 1*c*).

Behavior

Alloparental test. Males participated in a standard alloparental test (Cushing and Kramer, 2005a; Trainor et al., 2006; Young et al., 2005). Males were placed in an alloparental test arena consisting of two cages (12 × 18 × 28 cm) connected by a plastic tunnel. Males were allowed 30 min to adapt to the arena before a 1- to 3-d-old pup was placed in one of the two cages. The behavior of the male was videotaped and analyzed for 10 min after entrance into the pup's cage, or for 30 min if the male failed to enter the pup cage. Males that spent a minimum of 3 min in contact with the pup, licking and grooming, or huddling with the pup were classified as alloparental. Because all control males were alloparental, for the purpose of analysis they were grouped.

Social preference. Five days after the alloparental test, treated males were tested for social preference. This was done using the standardized vole partner preference test (Liu et al., 2001; Cushing et al., 2003). Treated males were cohabited with an unrelated sexually naive adult female for 1 h. This female was classified as the familiar "partner." Female prairie voles do not undergo spontaneous estrus and require prolonged exposure to a male to become sexually receptive. Therefore, mating is not a factor in this test. Immediately after cohabitation, test animals participated in a social preference test. The social preference arena consisted of three polycarbonate cages (12 × 18 × 28 cm) in a modified Y shape. The two cages housing stimulus animals were in parallel and a third cage (neutral) was attached separately to each stimulus cage. The familiar female was gently tethered in one of the stimulus cages while an age- and size-matched sexually naive female (novel/"stranger") that was unrelated to both the familiar female and the subject was tethered in the other stimulus cage. Then, the experimental male was placed in the neutral chamber and allowed to move about freely for 3 h. The test was recorded using a time-lapse video (12:1 ratio) and then scored by an experimentally blind scorer. The data scored and analyzed include frequency of entrance, total time spent in the chambers, and time spent in physical contact with partner and stranger. It should be noted that without hormonal manipulation, such as central administration of arginine vasopressin, 1 h of cohabitation does not lead to the formation of preference for the familiar stimulus animal (DeVries et al., 1996; Cho et al., 1999); therefore, control males were predicted to spend equal amounts of time in the cages of and in physical contact with both females.

Statistical analysis. Based on the a priori assumption that the two control groups would not differ, preplanned comparisons were made between the two controls. If and only if there was no difference in any measure, they were grouped into a single control group for the purpose of analysis, which was the case in this study. Alloparental data represents count data with two possible outcomes; therefore the data were analyzed using 2 × 2 Fisher's exact probability. For the social preference test, an ANOVA was used to analyze between treatment effects, whereas a paired *t* test was used for within-treatment analysis.

Results

As indicated by immunoreactivity of transfected ERα 12 (eight bilateral and four unilateral) of the 20 males in which AAV-ERα was injected into the MeA were successfully transfected (Fig. 1*a*). There were a total of 19 control males (9 MeA luciferase and 10 caudate ERα). There was a significant treatment effect of increased ERα in the MeA on both the expression of spontaneous alloparental behavior and social preference. Enhancing ERα in the MeA inhibited alloparental behavior with only 4 of 12 (33%) MeA-ERα males displaying alloparental behavior, compared with 19 of 19 (100%) of the control males (Fisher's exact $p < 0.0001$) (Fig. 2). Nonalloparental behavior displayed by MeA-ERα males included attacking the pup ($n = 5$), attempting to mount and mate with the pup ($n = 2$), or ignoring the pup ($n = 1$). As predicted, control males did not display a preference for either the familiar or novel female. In contrast, MeA-ERα males

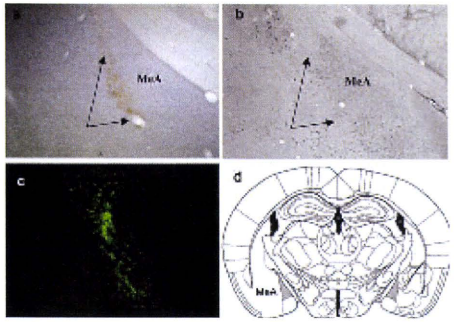

Figure 1. *a*, Photomicrograph of AAV-mediated ERα overexpression. *b*, Typical low levels of ERα immunoreactivity in the medial amygdala of male prairie voles. *c*, GFP expression. *d*, Graphic representation of the site of infusion (gray shaded area) (adapted from Paxinos and Franklin, 2001). Endogenous vole ERα (*a*) is labeled using the primary polyclonal antibody c1355 (Millipore; 1:10,000 dilution) and developed with nickel-DAB (purple staining) (Cushing et al., 2004), whereas transfected human ERα is labeled using the primary antibody RM9101-s (1:1000 dilution) and visualized using DAB (brown).

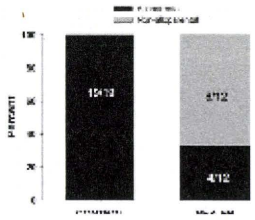

Figure 2. Results of treatment on the expression of spontaneous alloparental behavior. Enhancing EPα in the MeA (MeA-ERα) resulted in a significant decrease in alloparental behavior compared with control males. $p < 0.001$.

spent significantly more time in a novel female's cage compared with control males (ANOVA, $p < 0.05$) (Fig. 3). MeA-ERα males formed a "stranger" preference spending significantly more time in the cage of a novel female (pair *t* test, $p < 0.05$) and in physical contact with a novel female than with a familiar female (paired *t* test, $p < 0.05$) (Fig. 3).

Discussion

The results from this study indicate the importance of ERα in regulating male prosocial behavior providing direct evidence that ERα can inhibit the expression of male prosocial behavior. Furthermore, the results support the hypothesis that a reduction in ERα is necessary for the expression of high levels of male prosocial behavior. Increasing ERα in the MeA of the adult male prairie vole reduced or inhibited the expression of alloparental behavior and the initial formation of social preferences.

Unlike most male rodents, which are infanticidal or ignore pups, even inexperienced male prairie voles display high levels of spontaneous alloparental behavior, including licking, grooming, huddling, and retrieving unrelated pups. In the majority of males, enhancing ERα in the MeA produced a more "typical" male response that of pup-directed aggression, although in two males it produced a novel response: pup-directed sexual activity. The expression of spontaneous alloparental behavior is very difficult to disrupt in male prairie voles (Cushing and Kramer, 2005a), and although it has been suggested that alloparental behavior is controlled by neuropeptides, inhibition of endogenous neuropeptides does not disrupt the alloparental behavior in adult males. However, neonatal castration does disrupt male alloparental behavior (Lonstein et al., 2002) as well as significantly increasing ERα in the MeA (Cushing and Kramer, 2005b). These findings suggest that steroids play a major role in facilitating and perhaps organizing the male's response to pups. The fact that increasing ERα in adults and removal of testes from neonates both inhibit the expression of alloparental behavior suggests that a low threshold level of steroid is necessary for the expression of alloparental behavior, but that higher levels masculinize behavior.

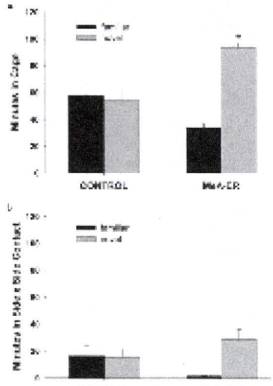

Figure 3. *a*, Mean time (± SE) that males spent in the cage of the familiar or novel female by treatment. *b*, Mean time (± SE) in side-by-side contact with the familiar and novel female by treatment. MeA-ERα males spent significantly less time in the familiar female cage and significantly more time in the novel female cage than control males ($p \leq 0.05$). Within-treatment analysis revealed that MeA-ERα males displayed a preference for the novel female spending significantly more time in the novel female cage than the familiar female cage, and more time in side-by-side contact with the novel female. *$p < 0.05$, significant between treatment difference; line above error bars shows significant difference within treatment, $p < 0.05$. Error bars indicate SEM.

Enhancing ERα in the MeA clearly altered alloparental behavior. However, there was variability in the response. Although the sample size was insufficient to determine the reason for the variability, it is possible that differential enhancement of ERα could explain part of the variation. Variation could have been related to unilateral versus bilateral enhancement of ERα. Although it has been hypothesized that the right and left amygdala may differentially regulate behavior (Cooke et al., 2007), empirical studies that have compared unilateral versus bilateral effects in the amygdala suggest that there is no difference as unilateral and bilateral lesions produce the same effect on behavior [MeA, Sheehan et al. (2001); basolateral, Floresco and Ghods-Sharifi (2007)]. Additionally, the degree of enhancement could have affected the response. It is possible that animals with more ERα responded differently than those with less. Finally, it could be a combination of the degree of enhancement and unilateral versus bilateral ERα. Future studies will be designed to determine whether the right and left side of the amygdala play different roles in regulating social behavior.

Although male prairie voles form long-term pair bonds, this process requires either extended cohabitation or central administration of the neuropeptide vasopressin (Insel and Young, 2001). Control males displayed the predicted response, spending an equal amount of time with the familiar and the novel female, whereas MeA-ERα males formed a preference for a novel female, spending significantly more time in contact with the novel female. This result is similar to observations of male mice in that after spending time with a nonreceptive female, males prefer a novel female when given a choice (Moy et al., 2004). The preference for a novel female is particularly relevant when considered in light of the numerous studies of social preference in prairie voles and the function of neuropeptides. In has been argued that neuropeptides are primarily responsible for the formation of pair bonds (Keverne and Curley, 2004; Young and Wang, 2004; Nair and Young, 2006). Vasopressin and oxytocin antagonists inhibited the formation of a partner preference or inhibited social contact, but did not result in the formation of a preference for a novel female (Cho et al., 1999). These results suggest that ERα expression significantly alters the normal steps involved in the formation of social preference. Interestingly, the only other study in which male prairie voles formed a preference for a novel female also involved steroidal manipulation through adrenalectomies followed by treatment with corticosterone (DeVries et al., 1996).

Although several mechanisms have been proposed to regulate the formation of pair bonds, the neuropeptide arginine vasopressin has been proposed to be the primary mechanism involved in regulating pair bond formation and parental behavior in male prairie voles (Young and Wang, 2004). Although we are not suggesting that the current results negate the role of vasopressin, they clearly demonstrate that there are critical aspects of social bonding that have not previously been investigated and that ERα plays a critical role. The results from this study bring into question the assumption that the pattern of the vasopressin V1a receptor (V1aR) is sufficient to explain the formation of pair bonds. Neonatal castration is one of the few reported methods to disrupt alloparental behavior in adult male prairie voles (Lonstein et al., 2002). Adult males that were castrated neonatally display a female pattern of ERα and females display low levels of alloparental behavior (Cushing and Kramer, 2005b). Neonatal castration also inhibited the subsequent ability of centrally administered vasopressin to stimulate partner preferences in adult males, but did not alter the expression of V1aR (Cushing et al., 2003), indicating that the lack of response was not caused by changes in the ability to respond to vasopressin. Chimeric male mice that express prairie vole V1aR display a prairie vole-like pattern of V1aR and an increase in general social affiliation (Young et al., 1999), but do not develop a partner/social preference. One possibility is that social preferences were absent in these transgenic mice because ERα expression was unchanged from the normal pattern, which includes high levels in the MeA. Prairie voles display variation in the length of a microsatellite in the V1aR promoter and length is positively correlated with the expression of prosocial behavior; additionally, this element in the V1aR of the polygynous montane and meadow voles is substantially shorter (Hammock and Young, 2004; Hammock et al., 2005). However, the assertion that the length of this microsatellite is the key element in prosocial behavior has recently been challenged with the finding that many other species in the genus *Microtus* that do not express high levels of social behavior also display significant variation in V1aR microsatellite length (Fink et al., 2006). This finding lead to the suggestion that other factors/genes must also be involved in the ultimate formation of long-term pair bonds. Although montane and meadow voles express the same V1aR microsatellite and the same pattern of V1aR in the brain, meadow voles display prosocial behavior in response to centrally administered vasopressin, whereas montane males do not (Young et al., 1999). They do, however, differ in ERα expression with meadow vole male expressing an intermediate pattern between montane and prairie (Cushing and Wynne-Edwards, 2006). We suggest that the current findings indicate that a reduction in ERα may also be necessary.

The formation of long-term social bonds is a complex process that has been proposed to involve at least two neural circuits, the social behavior neural circuit and the reward system (Young et al., 2005). It has been proposed that within these circuits the ventral pallidum (Lim et al., 2001) and lateral septum (Liu et al., 2001) play an essential role in pair bond formation in males, and the bed nucleus of the stria terminalis in male parental care (De Vries and Villalba, 1997). Here, we show that altering receptor patterns of a nucleus upstream of these regions is sufficient to alter the behavioral response to social stimuli. This does not negate the critical role of the lateral septum or reward system in the expression of social behavior, but clearly demonstrates that changes in the initial response to social stimuli can prevent potentiation of these areas. This also presents the possibility that variable responses can be produced from the same system by altering ERα expression, seasonally or otherwise, to change how the neural circuit regulates social behavior. The findings in this study do not imply that the MeA directly regulates pup-directed aggression or the formation of pair bonds, but that changing the receptor pattern can change the response of the whole circuit and dramatically alter the ultimate response. This conclusion is emphasized by the observation that MeA-ERα males mounted and thrust against the pup. Of the thousands of alloparental tests that have been run with prairie voles, this has never been reported, and supports the concept that altering receptor expression can result in misdirected behavior.

References

Cho MM, DeVries AC, Williams JR, Carter CS (1999) The effects of oxytocin and vasopressin on partner preferences in male and female prairie voles (*Microtus ochrogaster*). Behav Neurosci 113:1071–1079.

Clark KR, Liu X, McGrath JP, Johnson PR (1999) Highly purified recombinant adeno-associated virus vectors are biologically active and free of detectable helper and wild-type viruses. Hum Gene Ther 10:1031–1039.

Cooke BM, Stokas MR, Woolley CS (2007) Morphological sex differences and laterality in the prepubertal medial amygdala. J Comp Neurol 501:904–915.

Cushing BS, Kramer KM (2005a) Microtines: a model system for studying the evolution and regulation of social monogamy. Acta Theriol Sin 25:182–199.

Cushing BS, Kramer KM (2005b) Mechanisms underlying epigenetic effects of early social experience: the role of neuropeptides and steroids. Neurosci Biobehav Rev 29:1089–1115.

Cushing BS, Wynne-Edwards KE (2006) Estrogen receptor alpha distribution in male rodents is associated with social organization. J Comp Neurol 494:595–605.

Cushing BS, Okorie U, Young LJ (2003) The effects of early exposure of testosterone on the subsequent response of adult male prairie voles to arginine vasopressin. J Neuroendocrinol 15:1021–1026.

Cushing BS, Razzoli M, Murphy AZ, Epperson PM, Le WW, Hoffman GE (2004) Intraspecific variation in estrogen receptor alpha and the expression of male sociosexual behavior in two populations of prairie voles. Brain Res 1016:247–254.

DeVries AC, DeVries MB, Taymans SE, Carter CS (1996) The effects of stress on social preferences are sexually dimorphic in prairie voles. Proc Natl Acad Sci U S A 93:11980–11984.

De Vries GJ, Villalba C (1997) Brain sexual dimorphism and sex differences in parental and other social behaviors. Ann N Y Acad Sci 807:273–286.

Ferguson JN, Aldag JM, Insel TR, Young LJ (2001) Oxytocin in the medial amygdala is essential for social recognition in the mouse. J Neurosci 21:8278–8285.
Fink S, Excoffier L, Heckel G (2006) Mammalian monogamy is not controlled by a single gene. Proc Natl Acad Sci U S A 103:10955–10960.
Floresco SB, Ghods-Sharifi S (2007) Amygdala-prefrontal cortical circuitry regulates effort-based decision making. Cereb Cortex 17:251–260.
Hammock EA, Young LJ (2004) Functional microsatellite polymorphism associated with divergent social structure in vole species. Mol Biol Evo 21:1057–1063.
Hammock EA, Lim MM, Nair HP, Young LJ (2005) Association of vasopressin 1a receptor levels with a regulatory microsatellite and behavior. Genes Brain Behav 4:289–301.
Hnatczuk OC, Lisciotto CA, DonCarlos LL, Carter CS, Morrell JI (1994) Estrogen and progesterone receptor immunoreactivity (ER-IR and PR-IR) in specific brain areas of the prairie vole (*Microtus ochrogaster*) is altered by sexual receptivity and genetic sex. J Neuroendocrinol 6:89–100.
Insel TR, Young LJ (2001) The neurobiology of social attachment. Nat Rev Neurosci 2:129–136.
Keverne KB, Curley JP (2004) Vasopressin, oxytocin and social behaviour. Curr Opin Neurobiol 14:777–783.
Kramer KM, Simmons JL, Freeman DA (2008) Photoperiod alters central distribution of estrogen receptor α in brain regions that regulate aggression. Horm Behav 53:358–365.
Krezel W, Dupont S, Krust A, Chambon P, Chapman PF (2001) Increased anxiety and synaptic plasticity in estrogen receptor β-deficient mice. Proc Natl Acad Sci U S A 98:12278–12282.
Kudwa AE, Bodo C, Gustafsson JA, Rissman EF (2005) A previously uncharacterized role for estrogen receptor beta: defeminization of male brain and behavior. Proc Natl Acad Sci U S A 102:4608–4612.
Lim MM, Insel TR, Young LJ (2001) The ventral pallidum in the monogamous prairie vole: neuroanatomy and activity. Horm Behav 39:336–337.
Liu Y, Curtis JT, Wang ZX (2001) Vasopressin in the lateral septum regulates pair bond formation in male prairie voles (*Microtus ochrogaster*). Behav Neurosci 115:910–919.
Lonstein JS, Rood BD, De Vries GJ (2002) Parental responsiveness is feminized after neonatal castration in virgin male prairie voles, but not masculinized by perinatal testosterone in virgin females. Horm Behav 41:80–87.
Moy SS, Nadler JJ, Perez A, Barbaro RP, Johns JM, Magnuson TR, Piven J, Crawley JN (2004) Sociability and preference for social novelty in five inbred strains: an approach to assess autistic-like behavior in mice. Genes Brain Behav 3:287–302.
Musatov S, Chen W, Pfaff DW, Kaplitt MG, Ogawa S (2006) RNAi-mediated silencing of estrogen receptor {alpha} in the ventromedial nucleus of hypothalamus abolishes female sexual behaviors. Proc Natl Acad Sci U S A 103:10456–10460.
Nair HP, Young LJ (2006) Vasopressin and pair-bond formation: genes to brain to behavior. Physiology 21:146–152.
Newman SW (1999) The medial extended amygdala in male reproductive behavior. A node in the mammalian social behavior network. Ann N Y Acad Sci 877:242–257.
Ogawa S, Washburn TF, Taylor J, Lubahn DB, Korach KS, Pfaff DW (1998) Modifications of testosterone-dependent behaviors by estrogen receptor-alpha gene disruption in male mice. Endocrinology 139:5058–5069.
Paxinos G, Franklin KB (2001) The mouse brain in stereotaxic coordinates, Ed 2. San Diego: Academic.
Sheehan T, Paul M, Amaral E, Numan MJ, Numan M (2001) Evidence that the medial amygdala projects to the anterior/ventromedial hypothalamic nuclei to inhibit maternal behavior in rats. Neuroscience 106:341–356.
Trainor BC, Greiwe KM, Nelson RJ (2006) Individual differences in estrogen receptor a in select brain nuclei are associated with individual differences in aggression. Horm Behav 50:338–345.
Wersinger SR, Sannen K, Villalba C, Lubahn DB, Rissman EF, De Vries GJ (1997) Masculine sexual behavior is disrupted in male and female mice lacking a functional estrogen receptor alpha gene. Horm Behav 32:176–183.
Young LJ, Wang ZX (2004) The neurobiology of pair bonding. Nat Neurosci 7:1048–1054.
Young LJ, Nilsen R, Waymire KG, MacGregor GR, Insel TR (1999) Increased affiliative response to vasopressin in mice expressing the vasopressin receptor from a monogamous vole. Nature 400:766–768.
Young LJ, Murphy-Young AZ, Hammock EA (2005) Anatomy and neurochemistry of the pair bond. J Comp Neurol 493:51–57.

0013-7227/08/$15.00/0
Printed in U.S.A.

Endocrinology 149(2):802–811

doi: 10.1210/en.2007-0827

Gonadal Steroid Hormones Maintain the Stress-Induced Acetylcholine Release in the Hippocampus: Simultaneous Measurements of the Extracellular Acetylcholine and Serum Corticosterone Levels in the Same Subjects

Dai Mitsushima, Kenkichi Takase, Toshiya Funabashi, and Fukuko Kimura

Department of Physiology, Yokohama City University Graduate School of Medicine, Yokohama 236-0004, Japan

To examine the role of gonadal steroid hormones in the stress responses of acetylcholine (ACh) levels in the hippocampus and serum corticosterone levels, we observed these parameters simultaneously in intact, gonadectomized, or gonadectomized steroid-primed rats. In both sexes of rats, neither gonadectomy nor the replacement of gonadal steroid hormone affected the baseline levels of ACh. However, gonadectomy severely attenuated the stress response of ACh, whereas the replacement of corresponding gonadal hormone successfully restored the response to intact levels. The gonadal hormones affected the serum corticosterone levels in a different manner; the testosterone replacement in orchidectomized rats suppressed the baseline and the stress response of corticosterone levels, whereas the 17β-estradiol replacement in ovariectomized rats increased the levels. We further found that letrozole or flutamide administration in intact male rats attenuated the stress response of ACh. In addition, flutamide treatment increased the baseline levels of corticosterone, whereas letrozole treatment attenuated the stress response of corticosterone. Moreover, we found a low positive correlation between the ACh levels and corticosterone levels, depending on the presence of gonadal steroid hormone. We conclude that: 1) gonadal steroid hormones maintain the stress response of ACh levels in the hippocampus, 2) the gonadal steroid hormone independently regulates the stress response of ACh in the hippocampus and serum corticosterone, and 3) the sex-specific action of gonadal hormone on the cholinergic stress response may suggest a neonatal sexual differentiation of the septohippocampal cholinergic system in rats. (*Endocrinology* 149: 802–811, 2008)

SEPTOHIPPOCAMPAL CHOLINERGIC NEURONS play an important role in the formation of hippocampal-dependent memory (1–6). In behaving animals, extracellular acetylcholine (ACh) levels in the hippocampus are known to increase during stress (7–9) and learning (10–12). The released ACh not only enhances synaptic plasticity via the postsynaptic M_1 muscarinic receptors (13) but also is responsible for neurogenesis in the dentate gyrus (14). Moreover, the septohippocampal cholinergic inputs generate theta rhythm (15) that modulates the induction of long-term potentiation in the hippocampal CA1 neurons (16).

Although the role of the released ACh in the hippocampus has been mostly studied in male animals, we found the sex difference in the stress response of ACh in the hippocampus: immobilization stress acutely increased the extracellular ACh levels in the hippocampus, but the stress response of ACh in cycling female rats was significantly smaller than in males (17). The sex-specific cholinergic response could be attributed to the neonatal organizational effect of testosterone and/or the activational effects of gonadal steroid hormone. Although there is no evidence that sex neonatally differentiates the cholinergic system in rats, several findings strongly suggest activational effects of gonadal steroid hormones in the control of the septohippocampal cholinergic neurons: 1) 40–60% of cholinergic neurons in the septum possess estrogen receptor-α immunoreactivity in both sexes of rats (18, 19); 2) the number of choline acetyltransferase-immunoreactive neurons in the septum decreases after gonadectomy (18, 20) but is restored by testosterone (20) or 17β-estradiol replacement (21); and 3) circulating testosterone in male rats (22, 23) and 17β-estradiol in female rats (24–26) enhance memory consolidation. In the present study, therefore, to examine the activational effects of gonadal steroid hormones concerning sex difference in the stress response of ACh in the hippocampus, an *in vivo* microdialysis study was performed in intact, gonadectomized, or gonadectomized steroid-primed rats.

Exposure to stress also increases corticosterone release from adrenal cortex in a sex-specific manner (27–29). The increased circulating corticosterone not only controls the hippocampal pyramidal neurons (30) but also modulates memory consolidation in rats (31). Moreover, hippocampus partly mediates the negative feedback effect of corticosterone on the hypothalamic-pituitary-adrenal (HPA) axis (32–34). To further analyze the relation between extracellular ACh levels in the hippocampus and serum corticosterone levels in both sexes of rats, we observed these parameters simultaneously in the same subjects.

First Published Online October 25, 2007

Abbreviations: ACh, Acetylcholine; EIA, estradiol enzyme immunoassay; HPA, hypothalamic-pituitary-adrenal; PLSD, protected least significant difference.

***Endocrinology* is published monthly by The Endocrine Society (http://www.endo-society.org), the foremost professional society serving the endocrine community.**

Materials and Methods

Animals

Young male (239.5 ± 2.0 g) and female rats (176.8 ± 2.9 g) of the Wistar-Imamichi strain at 7–8 wk of age were obtained from Animal

Reproduction Research Co. (Omiya, Japan). Unisex groups of two to three rats were housed in plastic cages (length 31 cm, width 47 cm, height 20 cm) at a constant temperature of 23 ± 1 C under a constant cycle of light and dark (lights on from 0500 to 1900 h). Experiments were performed in an electromagnetic- and sound-shielded room (length 1.2 m, width 2.2 m, height 2.3 m) (27). Food and water were available *ad libitum* in all experimental periods. All the animal housing and surgical procedures were in accordance with the guidelines of the Institutional Animal Care and Use Committee of the Animal Research Center, Yokohama City University Graduate School of Medicine.

Experimental design

Experiment I. To examine the role of gonadal steroid hormones concerning sex difference in the stress response of ACh in the hippocampus, the two sexes were each divided into four groups. Male groups included: 1) gonadally intact male rats, 2) orchidectomized rats (group ORX), 3) orchidectomized 17β-estradiol-primed rats (group ORX+E), and 4) orchidectomized testosterone-primed rats (group ORX+T); female groups included: 1) gonadally intact diestrous female rats, 2) ovariectomized rats (group OVX), 3) ovariectomized 17β-estradiol-primed rats (group OVX+E), and 4) ovariectomized testosterone-primed rats (group OVX+T). Gonadectomy was performed 15.0 ± 1.6 d before the *in vivo* experiment, and a testosterone or 17β-estradiol capsule was sc implanted on the day of the gonadectomy. To make a 17β-estradiol capsule, we packed a 1:4 mixture of 17β-estradiol (Sigma, St. Louis, MO) and cholesterol crystals in a piece of SILASTIC brand tubing (15 mm length per 250 g body weight, inner diameter 2.0 mm, outer diameter 3.0 mm; Dow Corning, Midland, MI). To make a testosterone capsule, we packed testosterone crystals (Sigma) in a piece of SILASTIC brand tubing (30 mm length per 250 g body weight, inner diameter 2.0 mm, outer diameter 3.0 mm; Dow Corning). The packed capsules were soaked in saline for more than 24 h before use (35).

Four to six rats in each group were used for gonadal steroid hormone assay. The rats were deeply anesthetized with sodium pentobarbital and trunk blood was taken to determine the serum levels of 17β-estradiol and testosterone. Separated serum samples were stored at −70 C until 17β-estradiol and testosterone assay.

Experiment II. To specify the hormone pathway maintaining the cholinergic stress response, gonadally intact male rats were divided into three groups. The three groups of rats were orally administered an aromatase inhibitor (5 mg/kg·d; Letrozole, Novartis Pharma, East Hanover, NJ), an androgen receptor antagonist (15 mg/kg·d; Flutamide, Sigma), or a vehicle (0.2 ml of 4% carboxymethylcellulose) at 0900 h daily for 7 d, and the *in vivo* microdialysis study was performed on the seventh day.

Four rats in each group were used for gonadal steroid hormone assay. Trunk blood were taken as described in experiment I, and serum samples were stored at −70 C until the assay.

17β-Estradiol assay

The serum 17β-estradiol concentration was measured by estradiol enzyme immunoassay (EIA) kit (Cayman Chemical Co., Ann Arbor, MI). Before the assay, 500 μl of diethyl ether were mixed with 50 μl of serum sample and the supernatant evaporated. Then EIA buffer was added to reconstitute the sample for assay. Minimum detectability of the assay was 10.8 pg/ml in experiment I and 6.1 pg/ml in experiment II. The intraassay standard variation was 3.8%, and the interassay coefficient of variation was 8.2%.

Testosterone assay

The serum testosterone concentration was measured by testosterone EIA kit (Cayman). Before the assay, 500 μl of diethyl ether were mixed with 50 μl of serum sample and the supernatant evaporated. Then EIA buffer was added to reconstitute the sample for assay. Minimum detectability of the assay was 9.1 pg/ml in experiment I and 16.4 pg/ml in experiment II. The intraassay standard variation was 4.9%, and the interassay coefficient of variation was 8.7%.

In vivo microdialysis

Under anesthesia with sodium pentobarbital (30–50 mg/kg, ip), a stainless-steel guide cannula (outer diameter 0.52 mm) was implanted stereotaxically into the right side of the dorsal hippocampus. Coordinates were 3.2–3.5 mm anterior from the ear bar, 3.0 mm lateral to the midline, and 2.1–2.2 mm below the surface of the brain according to the brain atlas of Albe-Fessard *et al.* (36). The coordinates were adjusted based on sex and body weight (37). After the cannula implantation, a stylet was inserted into the guide cannula until the microdialysis experiment. The animals were housed individually and allowed to recover in a cylindrical plastic cage (diameter 35 cm, height 45 cm) for 10.2 ± 1.8 d. During this period, vaginal smears were taken to confirm expression of the normal estrous cycle in female rats. Male rats were handled for a short time daily.

On the day before the microdialysis experiment, the stylet was replaced with a microdialysis probe (outer diameter 0.31 mm, AI-8–1; Eicom Co., Kyoto, Japan), and a cardiac catheter was implanted through the jugular vein under light ether anesthesia. A two-channel fluid swivel device (SSU-20; Eicom) was connected to the inlet and outlet of the probe, and an artificial cerebrospinal fluid solution (147 mM NaCl; 4 mM KCl; 1.2 mM $CaCl_2$; 0.9 mM $MgCl_2$) was infused through the dialysis probe with a 1.0-mm-long semipermeable membrane (molecular mass cutoff 50,000 Da) at a rate of 2.5 μl/min using a microdialysis pump (CMA/102; Carnegie Medicin, Stockholm, Sweden). We administered 7 μM eserine through the dialysis probe to enhance the dialysate ACh levels. The rats were housed individually in their home cage, and the dialysis was performed under unanesthetized, freely moving conditions (27, 38, 39). After the stabilization period (overnight), the dialysates were collected (37.5 μl) in 15-min fractions for 5 h. After the collection of the first four samples, the immobilization stress was applied from 1200 to 1300 h, when the extracellular ACh levels were relatively stable (39, 40). In intact female rats, we collected dialysates on diestrous days (*i.e.* diestrus 1 or diestrus 2). Details of the immobilization and behavioral responses to the stress were described previously (27). We strapped the animals' legs onto a wooden board (19 × 30 cm) with soft cotton ties for 60 min.

At the same time, blood samples were taken from the same rats we described previously (35, 41). Blood (150 μl) was drawn twice before immobilization (at 1100 and 1200 h), twice during immobilization (at 1230 and 1300 h), and four times after release from immobilization (at 1330, 1400, 1500, and 1600 h). An equal volume of heparinized saline was replaced after each bleeding. Separated serum samples were stored at −70 C until corticosterone assay. After the sampling experiment, the animals were deeply anesthetized with sodium pentobarbital and perfused with 10% formalin solution. The location of the dialysis probe was microscopically verified in frozen sections of the brain (Fig. 1).

ACh assay

ACh was quantified by a combination of HPLC, enzyme reaction, and electrochemical detection (ECD-100; Eicom). Details of the ACh assay procedures were described previously (38–40). A 30-μl aliquot of dialysate was used for subsequent measurements of the ACh concentrations. Thirty microliters of ethylhomocholine solution (100 nM) were mixed with the aliquot for the internal standard solution, and the mixture was injected into the HPLC system. A solution that consisted of 0.1 mM Na_2HPO_4 (pH 8.5) containing 200 mg/liter sodium 1-decanesulfonate (Aldrich Chemical Co., Inc., Milwaukee, WI) and 65 mg/liter tetramethylammonium chloride (Wako Pure Chemical Industries Co., Osaka, Japan) was delivered to the HPLC as the mobile phase at a rate of 0.6 ml/min. After separation with a styrene polymer column (AC-GEL; Eicom), ACh was converted to hydrogen peroxide by a postcolumn enzyme reactor (AC-ENZYMPAK; Eicom) with immobilized acetylcholinesterase and choline oxidase. The hydrogen peroxide was detected with an electrochemical detector (ECD-100; Eicom). The least amount detected was 30–70 fmol/sample.

To calculate the recovery rate in each dialysis probe, *in vitro* experiments were also performed. The amount of ACh collected every 15 min was divided by the *in vitro* recovery rate to estimate extracellular ACh levels. The *in vitro* recovery rate was determined for individual probes and applied to results from individual rats (mean ± SEM; experiment I, 6.6 ± 0.3%, experiment II, 6.2 ± 0.2%).

Corticosterone assay

The serum corticosterone levels were determined by the protein-binding method (17, 27, 42, 43) in a single assay. Briefly, 1-ml ethanol was

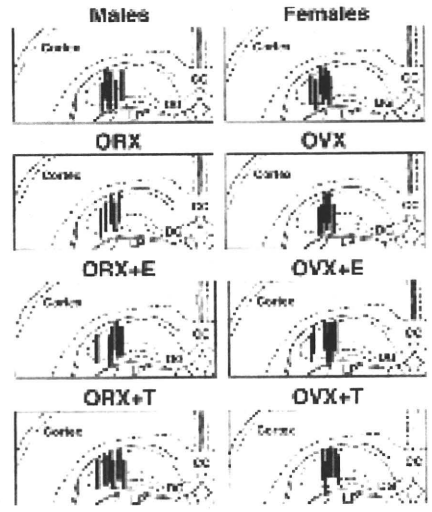

FIG. 1. Location of the microdialysis probes within the dorsal hippocampus. *Vertical lines* represent the 1.0 mm length of dialysis membrane. CC, Corpus callosum; DG, dentate gyrus; LP, lateral posterior nucleus.

mixed with 5 μl of serum sample and the supernatant evaporated. Then 1 ml of corticosterone-binding globulin-isotope solution was added to each tube. To make the corticosterone-binding globulin-isotope solution, 250 ml of 0.2% pooled human serum solution were filtrated and mixed with 5 μCi of 1,2,6,7-^{3}H-corticosterone (PerkinElmer Life Sciences, Inc., Boston, MA). An insoluble absorbing agent (Florisil; Wako Pure Chemical Industries) was used to separate protein-bound and unbound steroids. The minimal detectable amount of corticosterone was 2.3 μg/dl. The intraassay standard variation of the assay was 5.8%, and the intraassay coefficient of variation was 7.1%.

Data analysis

Serum 17β-estradiol and testosterone levels were analyzed by one-way ANOVA followed by *post hoc* analysis with the Fisher protected least significant difference (PLSD) test, in which the variable was the group. For time course analyses, extracellular ACh levels and serum corticosterone levels were analyzed by one-way ANOVA with repeated measures followed by *post hoc* analysis with the Fisher PLSD test, in which the variable was time.

Mean ACh levels or corticosterone levels before the stress exposure were defined as the baseline, and the stress-induced maximum levels during stress was defined as the stress response. In experiment I, to evaluate the sex difference in the baseline levels and the stress-induced levels, we performed three-way ANOVA, in which the variables were stress, sex, and hormone treatment. In experiment II, we performed two-way ANOVA, in which the variables were stress and drug treatment. The data were analyzed by *post hoc* ANOVAs with Fisher PLSD test to examine specific differences.

To examine the correlation between the ACh levels and serum corticosterone levels, eight points of ACh levels and serum corticosterone concentration (at 1100, 1200, 1230, 1300, 1330, 1400, 1500, and 1600 h) were evaluated by Pearson's correlation coefficient (38, 39). $P < 0.05$ was considered statistically significant.

Results

Serum concentration of 17β-estradiol and testosterone (experiment I)

Serum 17β-estradiol levels in experiment I are shown in Fig. 2A. The levels in ORX+E and OVX+E rats were equivalent to the peak levels in proestrous female rats (44, 45). In ANOVA followed by *post hoc* analysis, ORX+E rats showed significantly higher 17β-estradiol levels than male rats ($F_{3,13} = 12.176$, $P < 0.01$). In addition, OVX+E rats showed significantly higher, but OVX rats showed significantly lower, 17β-estradiol levels than diestrous female rats ($F_{3,14} = 18.043$, $P < 0.01$).

Serum testosterone levels in experiment I are shown in Fig. 2B. The levels in ORX+T and OVX+T rats were equivalent to the levels in intact male rats. Both ORX and ORX+E rats showed significantly lower testosterone levels than intact male rats ($F_{3,13} = 94.824$, $P < 0.01$). Similarly, both OVX and OVX+E rats showed significantly lower testosterone levels than diestrous female rats, and OVX+T rats showed significantly higher testosterone than diestrous female rats ($F_{3,14} = 27.434$, $P < 0.01$).

Time-course analysis in the extracellular ACh levels (experiment I)

In male groups, extracellular ACh levels increased rapidly at the onset of immobilization stress but gradually decreased thereafter, even before the immobilization ended. The ACh levels increased rapidly again after the end of immobilization stress and then dropped gradually when the animals were returned to their home cage (Fig. 3A). In gonadally intact male rats, ANOVA followed by *post hoc* analysis showed that the ACh levels during (at 1215, 1230, and 1245 h) and after (at 1315 and 1330 h) release from immobilization stress were significantly higher than the baseline levels before immobilization stress ($F_{16,80} = 9.953$, $P < 0.01$). Although the response duration was short in ORX rats ($F_{16,64} = 3.374$, $P < 0.01$), that was successfully restored by the replacement of either sex steroid (ORX+T, $F_{16,80} = 5.256$, $P < 0.01$; ORX+E, $F_{16,80} = 5.338$, $P < 0.01$).

Female groups showed a similar change in extracellular ACh levels, although the stress response of ACh was relatively low (Fig. 3B). In gonadally intact female rats, the ACh levels during (at 1215, 1230, and 1245 h) and after (at 1315 h) immobilization stress were significantly higher than the baseline levels ($F_{16,96} = 7.147$, $P < 0.01$). Although the response duration was short in

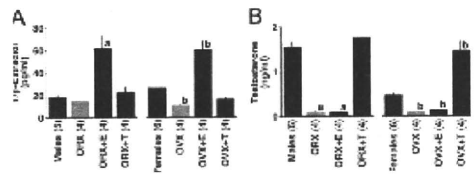

FIG. 2. A, Serum 17β-estradiol concentration in intact, gonadectomized, and gonadectomized steroid-primed rats. B, Serum testosterone concentration in intact, gonadectomized, and gonadectomized steroid-primed rats. SILASTIC brand capsule containing 17β-estradiol or testosterone was sc implanted for 2 wk in gonadectomized rats. Each data point represents the mean ± SEM. The number of rats in each group is shown in *parentheses*. a, $P < 0.05$ *vs.* males; b, $P < 0.05$ *vs.* females.

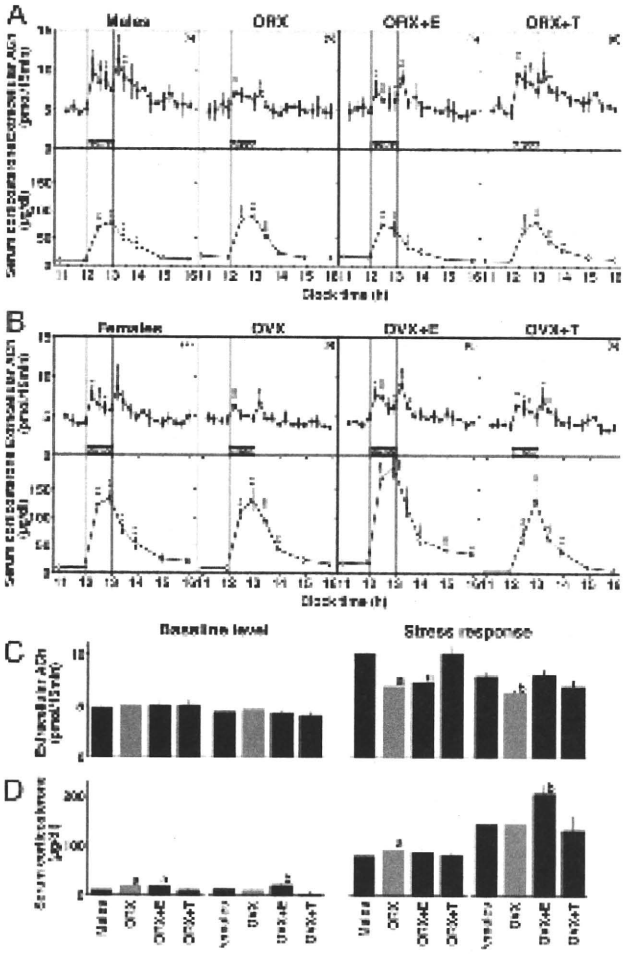

FIG. 3. A, Effects of orchidectomy and gonadal steroid hormone replacement on the stress response of extracellular ACh levels in the hippocampus and serum corticosterone levels in male rats. B, Effects of ovariectomy and gonadal steroid hormone replacement on the stress response of extracellular ACh levels in the hippocampus and serum corticosterone levels in female rats. *Horizontal black bars* indicate time of immobilization stress, and the *vertical gray lines* represent the onset and end of the immobilization. SILASTIC brand capsule containing 17β-estradiol or testosterone was sc implanted for 2 wk in gonadectomized rats. The number of rats in each group is shown in *parentheses*. *, $P < 0.05$; **, $P < 0.01$ *vs.* mean levels before immobilization stress. C, Gonadectomy significantly attenuated the stress response of ACh, whereas replacement of testosterone in ORX rats and 17β-estradiol in OVX rats restored the response. D, The baseline levels and stress response of serum corticosterone in the same subjects. a, $P < 0.05$ *vs.* males; b, $P < 0.05$ *vs.* females. All data are presented as means ± SEM.

OVX rats ($F_{16,80} = 5.602$, $P < 0.01$), that was successfully restored by the replacement of either sex steroid (OVX+T, $F_{16,80} = 7.290$, $P < 0.01$; OVX+E, $F_{16,112} = 10.773$, $P < 0.01$).

Group comparison in the extracellular ACh levels (experiment I)

The baseline levels and the stress-induced ACh levels were analyzed using three-way ANOVA (Fig. 3C). Main effects of stress ($F_{1,84} = 124.685$, $P < 0.01$) and sex ($F_{1,84} = 13.783$, $P < 0.01$) were significant. Interactions in stress *vs.* hormone ($F_{3,84} = 4.345$, $P < 0.01$), stress *vs.* sex ($F_{1,84} = 4.313$, $P < 0.01$), and stress *vs.* sex *vs.* hormone ($F_{3,84} = 3.202$, $P < 0.05$) were also statistically significant.

Post hoc ANOVAs with Fisher PLSD test showed that orchidectomy severely attenuated the stress response of ACh, which was successfully restored by testosterone replacement. However, 17β-estradiol replacement did not restore the stress response of ACh in ORX rats. The stress response of ACh in ORX or ORX+E rats was significantly less than in intact male or ORX+T rats ($P < 0.01$). The baseline levels of ACh were not statistically different.

In female groups, the stress response of ACh was relatively low, and gonadally intact rats showed significant sex difference ($P < 0.05$). Ovariectomy severely attenuated the stress response of ACh, but 17β-estradiol replacement successfully restored the response in OVX rats. Testosterone replacement may partially restore the response in OVX rats, but the stress response of ACh in OVX+T rats was not different from that in OVX rats. The stress response of ACh in OVX rats was significantly less than in diestrous female or OVX+E rats ($P < 0.05$). The baseline levels of ACh were not statistically different.

Time-course analysis in the serum corticosterone levels (experiment I)

In male groups, serum corticosterone levels increased clearly upon exposure to immobilization stress (Fig. 3A). ANOVA followed by *post hoc* analysis showed that the corticosterone levels during and after release from immobilization were significantly higher than the baseline levels (males, $F_{6,30} = 40.842$, $P < 0.01$; ORX, $F_{6,24} = 40.936$, $P < 0.01$; ORX+T, $F_{6,30} = 35.807$, $P < 0.01$; ORX+E, $F_{6,30} = 16.616$, $P < 0.01$).

In all female groups, the stress response of serum corticosterone was relatively high (Fig. 3B). Although similar stress response of corticosterone was observed in diestrous female ($F_{6,36} = 36.328$, $P < 0.01$), OVX ($F_{6,30} = 12.925$, $P < 0.01$), and OVX+T rats ($F_{6,30} = 14.130$, $P < 0.01$), OVX+E rats showed longer response duration ($F_{6,42} = 31.301$, $P < 0.01$).

Group comparison in the serum corticosterone levels (experiment I)

The baseline levels and stress-induced corticosterone levels were analyzed using three-way ANOVA (Fig. 3D). Main effects of stress ($F_{1,84} = 457.546$, $P < 0.01$), sex ($F_{1,84} = 43.712$, $P < 0.01$), and hormone ($F_{3,84} = 5.920$, $P < 0.01$) were statistically significant. Interactions in stress *vs.* sex ($F_{1,84} = 51.868$, $P < 0.01$), sex *vs.* hormone ($F_{3,84} = 5.366$, $P < 0.01$), and stress *vs.* sex *vs.* hormone ($F_{3,84} = 3.840$, $P < 0.05$) were also statistically significant.

In *post hoc* ANOVA with Fisher PLSD test, ORX and ORX+E rats showed significantly higher baseline levels of corticosterone than male and ORX+T rats ($P < 0.05$). Moreover, ORX rats showed significantly higher stress response of corticosterone than male and ORX+T rats ($P < 0.05$).

OVX+E rats showed significantly higher baseline levels of corticosterone than diestrous female, OVX, and OVX+T rats ($P < 0.01$). In addition, OVX+E rats showed significantly higher stress response of corticosterone than diestrous female, OVX, and OVX+T rats ($P < 0.05$). Diestrous female rats showed significantly higher response than intact male rats ($P < 0.01$).

Correlation between the ACh levels and serum corticosterone levels (experiment I)

The extracellular ACh levels showed a weak positive correlation with the serum corticosterone levels in intact male and female rats (Table 1). Although gonadectomy attenuated the correlation in both sexes of rats, treatment with either 17β-estradiol or testosterone restored the weak correlation.

TABLE 1. Correlation between the extracellular ACh levels and serum corticosterone levels in intact, gonadectomized, and gonadectomized steroid-primed rats

Group	No. of animals	No. of data points	Correlation (r)	*P* value
Males	6	48	0.361	0.011[a]
ORX	5	40	0.281	0.078
ORX+E	6	48	0.391	0.006[a]
ORX+T	6	48	0.369	0.009[a]
Females	7	56	0.306	0.021[a]
OVX	6	48	0.036	0.812
OVX+E	8	64	0.331	0.007[a]
OVX+T	6	48	0.327	0.023[a]

[a] Statistically significant correlation.

Serum concentration of 17β-estradiol and testosterone in letrozole- or flutamide-treated male rats (experiment II)

For experiment II, serum 17β-estradiol and testosterone levels are shown in Fig. 4, A and B, respectively. Daily treatment with letrozole significantly decreased 17β-estradiol levels in male rats ($F_{2,9} = 6.247$, $P < 0.05$). In addition, treatment with either letrozole or flutamide significantly increased testosterone levels ($F_{2,9} = 152.295$, $P < 0.01$). Flutamide-treated rats showed significantly higher testosterone levels than letrozole-treated rats.

Time-course analysis in the extracellular ACh levels in letrozole- or flutamide-treated male rats (experiment II)

Extracellular ACh levels increased rapidly with the onset of immobilization stress (Fig. 5A). Vehicle-treated rats showed a clear change as observed in experiment I ($F_{16,80} = 6.604$, $P < 0.01$). Letrozole-treated rats showed small response and short-response duration ($F_{16,80} = 4.694$, $P < 0.01$). Flutamide-treated rats showed small ACh response to stress ($F_{16,96} = 7.271$, $P < 0.01$).

Group comparison in the extracellular ACh levels (experiment II)

The baseline levels and the stress-induced ACh levels were analyzed using two-way ANOVA (Fig. 5B). Main effects of stress ($F_{1,32} = 71.351$, $P < 0.01$) and treatment ($F_{2,32} = 5.899$, $P < 0.01$) were significant. Interaction in stress *vs.* treatment

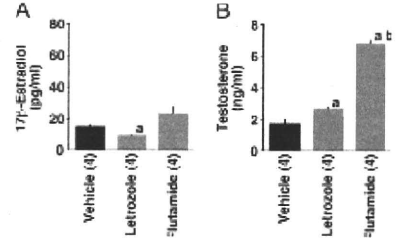

FIG. 4. Serum 17β-estradiol (A) and testosterone (B) concentration in vehicle-, letrozole-, and flutamide-treated male rats. Rats were orally administered vehicle, letrozole (5 mg/kg·d), or flutamide (15 mg/kg·d) for 1 wk. Each data point represents the mean ± SEM. The number of rats in each group is shown in *parentheses*. a, $P < 0.05$ *vs.* vehicle; b, $P < 0.05$ *vs.* letrozole.

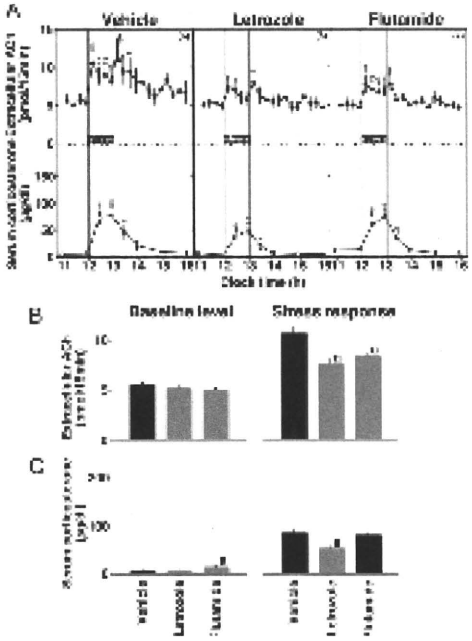

FIG. 5. A, Effects of letrozole or flutamide on the stress response of extracellular ACh levels in the hippocampus and serum corticosterone levels in gonadally intact male rats. *Horizontal black bars* indicate timing of immobilization stress, and the *vertical gray lines* represent the onset and end of the immobilization. Rats were orally administered vehicle, letrozole (5 mg/kg·d), or flutamide (15 mg/kg·d) for 1 wk. The number of rats in each group is shown in *parentheses*. *, $P < 0.05$; **, $P < 0.01$ *vs.* mean levels before immobilization stress. B, Both letrozole and flutamide treatment significantly attenuated the stress response of ACh. C, The baseline levels and stress response of serum corticosterone in the same subjects. a, $P < 0.05$ *vs.* vehicle. All data are presented as means ± SEM.

($F_{2,32} = 4.345$, $P < 0.01$) was also statistically significant. In *post hoc* ANOVA with Fisher PLSD test, treatment with either letrozole or flutamide significantly attenuated the stress response of ACh ($P < 0.05$).

Time-course analysis in serum corticosterone levels in letrozole- or flutamide-treated male rats (experiment II)

In all groups, the serum corticosterone levels increased clearly upon exposure to immobilization stress (Fig. 5A). Although the stress response of corticosterone in vehicle- or flutamide-treated rats was similar to the response in intact male rats (vehicle, $F_{6,30} = 21.676$, $P < 0.01$; flutamide, $F_{6,36} = 43.206$, $P < 0.01$), the stress response was small in letrozole-treated rats ($F_{6,30} = 23.209$, $P < 0.01$).

TABLE 2. Correlation between the extracellular ACh levels and serum corticosterone levels in letrozole- or flutamide-treated male rats

Group	No. of animals	No. of data points	Correlation (r)	*P* value
Vehicle	6	48	0.399	0.005[a]
Letrozole	6	48	0.339	0.018[a]
Flutamide	7	56	0.385	0.003[a]

[a] Statistically significant correlation.

Group comparison in the serum corticosterone levels (experiment II)

The baseline levels and stress-induced corticosterone levels were analyzed using two-way ANOVA (Fig. 5C). Main effect of stress ($F_{1,32} = 316.359$, $P < 0.01$) and treatment ($F_{2,32} = 10.252$, $P < 0.01$) was significant. Interaction in stress *vs.* treatment ($F_{2,32} = 6.442$, $P < 0.01$) was also statistically significant. In *post hoc* ANOVA with Fisher PLSD test, flutamide treatment significantly increased the baseline levels of corticosterone ($P < 0.01$). In contrast, letrozole treatment significantly attenuated the stress response of corticosterone ($P < 0.01$).

Correlation between the ACh levels and serum corticosterone levels (experiment II)

The extracellular ACh levels consistently showed a weak positive correlation with serum corticosterone levels in experiment II (Table 2). Neither letrozole nor flutamide treatment affected the weak correlation.

Discussion

In experiment I, we found severe impairment of the stress response of ACh in the hippocampus after gonadectomy. The replacement of testosterone in ORX rats and the replacement of 17β-estradiol in OVX rats successfully restored the sex-specific ACh response and the duration of the response. The sex-specific action of gonadal hormone on the cholinergic stress response may suggest a neonatal sexual differentiation of the septohippocampal cholinergic system in rats.

Although stress-induced ACh increase has not been hitherto studied in gonadectomized steroid-primed rats, our results are consistent with previous neuroanatomical and neurochemical findings. Neuroanatomically, orchidectomy decreases the density of cholinergic fibers in the hippocampus, whereas testosterone replacement in ORX rats maintains fiber density in rats (20). Moreover, cholinergic neurons mediate the estradiol-induced increase in *N*-methyl-D-aspartate receptor binding in the hippocampus and CA1 spine density in female rats (46, 47). Neurochemically, 17β-estradiol increases the induction of choline acetyltransferase in the basal forebrain in OVX rats (48, 49). An *in vitro* study also demonstrated that treatment with 17β-estradiol increases both high-affinity choline uptake and ACh synthesis in basal forebrain neurons (50). Despite all this evidence suggesting the activational effect of sex hormones on ACh release in the hippocampus, the conclusive evidence such as the physiological release response has been lacking in behaving animals. Our results provide the first evidence that the stress response of ACh is dependent on the presence of gonadal steroid hormones in rats.

Nevertheless, 17β-estradiol replacement was unable to restore the stress response of ACh in ORX rats. Consistently, estradiol treatment failed to increase the amount of *N*-methyl-D-aspartate receptor binding (51) and spine density in the CA1 area in ORX rats (52). In female rats, testosterone replacement in OVX rats failed to raise the stress response of ACh up to the levels seen in ORX+T rats. Moreover, in our preliminary study, the replacement of androgen receptor agonist (5α-dihydrotestosterone) in OVX rats failed to enhance the cholinergic response (6.6 ± 0.3 pmol per 15 min, n = 7). These results, together with the present study suggest that the corresponding gonadal steroid hormone maintains the stress response of ACh and that the sex-specific action of gonadal steroid hormone is due to the neonatal sexual differentiation rather than the activational effect of gonadal steroid hormone in adult rats.

What is the physiological relevance of the stress response of ACh in the hippocampus? As mentioned in the introductory text, behavioral studies demonstrated that the extracellular ACh level in the hippocampus increases during the learning period (10–12) and is positively correlated with memory functions (53, 54). At the cellular level, both pyramidal and non-pyramidal neurons in the hippocampal CA1 area receive direct cholinergic afferents mediated by the muscarinic receptors (55–57). Moreover, the released ACh in the hippocampus not only enhances synaptic plasticity via the postsynaptic M_1 muscarinic receptors (13) but is also responsible for neurogenesis in the dentate gyrus (14, 58). Considering the acute stress response of ACh, enhancement of memory consolidation might be useful to anticipate similar crises in the future. In support of this, the endogenous ACh in the hippocampus is known to play an important role in the encoding of contextual episodes in fear conditioning tests: bilateral injections of scopolamine or selective M_1 receptor antagonist into the hippocampus impair the contextual freezing response in male rats (6, 59), and genetic deficiency of M_1 receptor reduces the freezing response in male mice (60). Although it is unclear whether this notion is applicable to humans, many people remember where they were and what they were doing when stressful events occur (61).

Male rats show a greater stress response of ACh than female rats (17), which seems to be consistent with the greater memory retention of male rats in contextual fear conditioning tests (27, 62). Moreover, in male rats, orchidectomy impairs memory consolidation for contextual fear, whereas testosterone injection restores the freezing response (63). In female mice, orchidectomy also impairs the contextual freezing response, whereas treatment with estradiol benzoate increases the response (64). Although there is some debate about the role of estrogen during stressful times (65), septohippocampal cholinergic neurons may be responsible for the mnemonic effect of testosterone (22, 23) and 17β-estradiol (24–26).

Cytochrome P450 aromatase, which converts testosterone to 17β-estradiol, is abundantly expressed in the basal forebrain (66, 67). Because testosterone replacement successfully restored the stress response of ACh in ORX rats, we hypothesized that the androgen and/or the estrogen receptors contribute to maintain the stress response of ACh in male rats. It was suggested that subcutaneous treatment of letrozole or flutamide crosses the blood-brain barrier, changing the CA1 spine synapse density in rats (68, 69). In addition, behavioral analysis suggests that peripherally administered flutamide influences central structures through interactions with androgen receptors (70), and high radioactivity was found in the cerebrum after a single oral administration of ^{14}C-letrozole in rats (Novartis AG, unpublished data). In experiment II, we found that letrozole attenuated the stress response of ACh, suggesting that inhibition of the 17β-estradiol production attenuated the cholinergic response in male rats. Because letrozole treatment significantly increased serum testosterone levels but decreased serum 17β-estradiol levels in male rats, activation of androgen receptor alone may not be sufficient to maintain the cholinergic response. Moreover, our preliminary results showed that the replacement of the nonaromatizable form of testosterone (5α-dihydrotestosterone) in ORX rats did not restore the cholinergic response; the stress-induced ACh increase in 5α-dihydrotestosterone-primed ORX rats was 7.6 ± 0.5 pmol (per 15 min, n = 6), which was identical with the response in ORX or ORX+E rats.

These results seem consistent with the observation that testosterone but not 5α-dihydrotestosterone improves working memory in aged male rats (71). It is also possible that elevated serum testosterone by letrozole down-regulates the expression of androgen receptor mRNA as observed in many target tissues (72). Although the effect is unknown in septohippocampal cholinergic neurons, exogenous testosterone may not down-regulate the expression in cholinergic motoneurons in male hamsters (73). In contrast, activation of estrogen receptors alone may not be sufficient to maintain the cholinergic response because flutamide treatment also attenuated the stress response of ACh. This notion is also supported by the results of ORX+E rats in experiment I. Taken together, these findings led us to the hypothesis that a combination of both androgen and estrogen receptors mediates the action of testosterone in maintaining the stress response in male rats. To prove the hypothesis, further study is necessary to examine the cholinergic stress response in ORX rats after the combined replacement of 5α-dihydrotestosterone and low dose of estrogen.

Neuroanatomical studies demonstrated that approximately 60% of septal cholinergic neurons express the estrogen receptor-α in male rats (19), whereas fewer cholinergic neurons express the androgen receptors in the septum and diagonal band of Broca (20). Therefore, it is possible that aromatized testosterone (*i.e.* 17β-estradiol) may directly activate the septohippocampal cholinergic neurons, whereas nonaromatized testosterone may transsynaptically activate the cholinergic neurons in male rats. Furthermore, gonadectomized rats showed small but significant stress response of ACh, which appeared to be sex hormone independent. Although the mechanism is presently unknown, significant localization of the cytochromes P45017α and P450 aromatase was demonstrated in the hippocampus and hypothalamus in adult male rats (74). Using Western immunoblot analysis, they reported that the concentration of P45017α and P450 aromatase in the hippocampus was approximately 1/100th to 1/200th the levels in the testis (P45017α) and ovary (P450 aromatase). It is possible, therefore, that the brain-derived sex hormones from endogenous cholesterol are associated with the sex hormone-independent component in gonadectomized rats.

In the serum corticosterone levels, increased stress response in ORX rats was attenuated by the testosterone replacement, which is consistent with previous reports (28, 75, 76). Furthermore, activation of androgen receptor alone by letrozole treat-

ment attenuated the stress response of corticosterone in male rats. These results may suggest that androgen receptor contributes to the suppression of the HPA axis in male rats. In contrast, 17β-estradiol replacement in OVX rats increased the baseline and the stress response of serum corticosterone as reported previously (77–79). However, in the present study, 17β-estradiol treatment in ORX rats did not enhance the corticosterone response up to the levels seen in female rats. Moreover, testosterone treatment did not attenuate the response in OVX rats. Although the reason is presently unknown, the difference in the stressor and/or the strain of rats may be associated with the issue.

Thus, the effects of gonadectomy and the replacement of gonadal steroid hormone on corticosterone response to stress were different from those on ACh response, suggesting the mechanism of gonadal steroid hormone action on the HPA axis is different from that on the septohippocampal cholinergic neurons. Although the neural mechanism of how gonadal steroid hormone affect the HPA axis has been unclear, androgen inhibits the expression of c-*fos* and CRH mRNA in the paraventricular nucleus of the hypothalamus in ORX rats (80). In OVX rats, a recent report suggested that 17β-estradiol does not enhance the expression of c-*fos* and CRH mRNA but increases adrenal gland sensitivity to ACTH (81).

Based on pharmacological and behavioral studies, the corticosterone response to various stressors affects memory consolidation (82–85). For example, systemic injections of moderate doses of corticosterone enhance memory function (86–88), whereas long-term exposure to high doses of corticosterone impairs it (89). Considering the inverted-U-shaped relationship between stress and learning (90), it is possible that moderate corticosterone response in male rats has a mnemonic effect, whereas greater corticosterone response in female rats has an amnesic effect. However, this notion may be difficult to explain the testosterone- or the 17β-estradiol-induced enhancement of memory consolidation in gonadectomized rats (22–26).

In the present study, ACh levels in the hippocampus and serum corticosterone levels were simultaneously monitored in the same subjects because an inhibitory role of the hippocampus on the HPA axis has been suggested in gonadally intact animals (32–34). Moreover, both ACh and corticosterone directly regulate the CA1 pyramidal neurons (30, 55), in which corticosterone affects the carbachol-evoked depolarization rather than its effect on the synaptic potentials and after hyperpolarization (91). Although we hypothesized that cholinergic activation of the hippocampus may inhibit the stress response of the HPA axis in intact rats (17), no inverse relation between the ACh levels in the hippocampus and serum corticosterone levels was observed in gonadectomized steroid-primed rats. We found only a low positive correlation between the ACh levels and corticosterone levels, depending on the presence of gonadal steroid hormone (Tables 1 and 2). The present results seem to be consistent with the observation that a selective immunotoxic lesion of septohippocampal cholinergic neurons does not affect circulating corticosterone levels in male rats (92). In addition, circulating corticosterone may not affect the ACh levels because the administration of exogenous corticosterone did not change the extracellular ACh levels in the hippocampus (7). These findings, together with the present study, suggest that the activation of septohippocampal cholinergic neurons may have little effect on the corticosterone response to stress, whereas increase in serum corticosterone may not affect the cholinergic response to stress. Although the activation of adrenocorticosteroid receptors in the hippocampal pyramidal neurons (90) may participate in the negative feedback regulation of the HPA axis (32, 93), cholinergic activation of the hippocampus seems to play a different role during stress.

Acknowledgments

The authors thank Kai Yamanashi for critical comments on this manuscript and Novartis Pharma AG for the generous gift of letrozole.

Received June 20, 2007. Accepted October 16, 2007.

Address all correspondence and requests for reprints to: Dai Mitsushima, D.V.M., Ph.D., Department of Neuroendocrinology, Yokohama City University Graduate School of Medicine, Yokohama 236-0004, Japan. E-mail: dm650314@med.yokohama-cu.ac.jp.

This work was supported by Grant-in-Aid 18590219 from the Ministry of Education, Culture, Sports, Science, and Technology of Japan (to D.M.).

Disclosure Statement: The authors have nothing to declare.

References

1. **Brito GN, Davis BJ, Stopp LC, Stanton ME** 1983 Memory and the septo-hippocampal cholinergic system in the rat. Psychopharmacology 81:315–320
2. **Izquierdo I, da Cunha C, Rosat R, Jerusalinsky D, Ferreira MB, Medina JH** 1992 Neurotransmitter receptors involved in post-training memory processing by the amygdala, medial septum, and hippocampus of the rat. Behav Neural Biol 58: 16–26
3. **Carli M, Luschi R, Samanin R** 1997 Dose-related impairment of spatial learning by intrahippocampal scopolamine: antagonism by ondansetron, a 5-HT_3 receptor antagonist. Behav Brain Res 82:185–194
4. **Ohno M, Kobayashi M, Kishi A, Watanabe S** 1997 Working memory failure by combined blockade of muscarinic and β-adrenergic transmission in the rat hippocampus. Neuroreport 8:1571–1575
5. **Gale GD, Anagnostaras SG, Fanselow MS** 2001 Cholinergic modulation of Pavlovian fear conditioning: effects of intrahippocampal scopolamine infusion. Hippocampus 11:371–376
6. **Wallenstein GV, Vago DR** 2001 Intrahippocampal scopolamine impairs both acquisition and consolidation of contextual fear conditioning. Neurobiol Learn Mem 75:245–252
7. **Imperato A, Puglisi-Allegra S, Casolini P, Angelucci L** 1991 Changes in brain dopamine and acetylcholine release during and following stress are independent of the pituitary-adrenocortical axis. Brain Res 538:111–117
8. **Tajima T, Endo H, Suzuki Y, Ikari H, Gotoh M, Iguchi A** 1996 Immobilization stress-induced increase of hippocampal acetylcholine and of plasma epinephrine, norepinephrine and glucose in rats. Brain Res 13:155–158
9. **Mizuno T, Kimura F** 1997 Attenuated stress response of hippocampal acetylcholine release and adrenocortical secretion in aged rats. Neurosci Lett 222:49–52
10. **Ragozzino ME, Unick KE, Gold PE** 1996 Hippocampal acetylcholine release during memory testing in rats: augmentation by glucose. Proc Natl Acad Sci USA 93:4693–4698
11. **Stancampiano R, Cocco S, Cugusi C, Sarais L, Fadda F** 1999 Serotonin and acetylcholine release response in the rat hippocampus during a spatial memory task. Neuroscience 89:1135–1143
12. **Hironaka N, Tanaka K, Izaki Y, Hori K, Nomura M** 2001 Memory-related acetylcholine efflux from the rat prefrontal cortex and hippocampus: a microdialysis study. Brain Res 901:143–150
13. **Shinoe T, Matsui M, Taketo MM, Manabe T** 2005 Modulation of synaptic plasticity by physiological activation of M_1 muscarinic acetylcholine receptors in the mouse hippocampus. J Neurosci 25:11194–11200
14. **Mohapel P, Leanza G, Kokaia M, Lindvall O** 2005 Forebrain acetylcholine regulates adult hippocampal neurogenesis and learning. Neurobiol Aging 26:939–946
15. **Lee MG, Chrobak JJ, Sik A, Wiley RG, Buzsáki G** 1994 Hippocampal θ activity following selective lesion of the septal cholinergic system. Neuroscience 62:1033–1047
16. **Hyman JM, Wyble BP, Goyal V, Rossi CA, Hasselmo ME** 2003 Stimulation in hippocampal region CA1 in behaving rats yields long-term potentiation when delivered to the peak of theta and long-term depression when delivered to the trough. J Neurosci 23:11725–11731
17. **Mitsushima D, Masuda J, Kimura F** 2003 Sex differences in the stress-induced release of acetylcholine in the hippocampus and corticosterone from the adrenal cortex in rats. Neuroendocrinology 78:234–240
18. **Mufson EJ, Cai WJ, Jaffar S, Chen E, Stebbins G, Sendera T, Kordower JH** 1999 Estrogen receptor immunoreactivity within subregions of the rat forebrain: neuronal distribution and association with perikarya containing choline acetyltransferase. Brain Res 849:253–274
19. **Miettinen RA, Kalesnykas G, Koivisto EH** 2002 Estimation of the total number of cholinergic neurons containing estrogen receptor-α in the rat basal forebrain. J Histochem Cytochem 50:891–902
20. **Nakamura N, Fujita H, Kawata M** 2002 Effects of gonadectomy on immunoreactivity for choline acetyltransferase in the cortex, hippocampus, and basal forebrain of adult male rats. Neuroscience 109:473–485
21. **Gibbs RB, Pfaff DW** 1992 Effects of estrogen and fimbria/fornix transection on p75NGFR and ChAT expression in the medial septum and diagonal band of Broca. Exp Neurol 116:23–39
22. **Kritzer MF, McLaughlin PJ, Smirlis T, Robinson JK** 2001 Gonadectomy impairs T-maze acquisition in adult male rats. Horm Behav 39:167–174
23. **Gibbs RB** 2005 Testosterone and estradiol produce different effects on cognitive performance in male rats. Horm Behav 48:268–277
24. **Daniel JM, Fader AJ, Spencer AL, Dohanich GP** 1997 Estrogen enhances performance of female rats during acquisition of a radial arm maze. Horm Behav 32:217–225
25. **Markowska AJ, Savonenko AV** 2002 Effectiveness of estrogen replacement in restoration of cognitive function after long-term estrogen withdrawal in aging rats. J Neurosci 22:10985–10995
26. **Luine V, Jacome LF, MacLusky NJ** 2003 Rapid enhancement of visual and place memory by estrogens in rats. Endocrinology 144:2836–2844
27. **Mitsushima D, Yamada K, Takase K, Funabashi T, Kimura F** 2006 Sex differences in the basolateral amygdala: the extracellular levels of serotonin and dopamine and their responses to restraint stress in rats. Eur J Neurosci 24:3245–3254
28. **Seale JV, Wood SA, Atkinson HC, Harbuz MS, Lightman SL** 2004 Gonadal steroid replacement reverses gonadectomy-induced changes in the corticosterone pulse profile and stress-induced hypothalamic-pituitary-adrenal axis activity of male and female rats. J Neuroendocrinol 16:989–998
29. **Kitay JI** 1961 Sex differences in adrenal cortical secretion in the rat. Endocrinology 68:818–824
30. **Nishi M, Usuku T, Itose M, Fujikawa K, Hosokawa K, Matsuda KI, Kawata M** 2007 Direct visualization of glucocorticoid receptor positive cells in the hippocampal regions using green fluorescent protein transgenic mice. Neuroscience 146: 1555–1560
31. **Roozendaal B** 2002 Stress and memory: opposing effects of glucocorticoids on memory consolidation and memory retrieval. Neurobiol Learn Mem 78:578–595
32. **McEwen BS, Weiss JM, Schwartz LS** 1968 Selective retention of corticosterone by limbic structures in rat brain. Nature 220:911–912
33. **Herman JP, Schäfer MKH, Young EA, Thompson R, Douglass J, Akil H, Watson SJ** 1989 Evidence for hippocampal regulation of neuroendocrine neurons of the hypothalamo-pituitary-adrenocortical axis. J Neurosci 9:3072–3082
34. **Sapolsky RM, Zola-Morgan S, Squire LR** 1991 Inhibition of glucocorticoid secretion by the hippocampal formation in the primate. J Neurosci 11:3695–3704
35. **Tin-Tin-Win-Shwe, Mitsushima D, Shinohara K, Kimura F** 2004 Sexual dimorphism of GABA release in the medial preoptic area and luteinizing hormone release in gonadectomized estrogen-primed rats. Neuroscience 127:243–250
36. **Albe-Fessard D, Stutinsky F, Libouban S** 1966 Atlas stéréotaxique du diencéphale de rat blanc. Paris: Centre National de la Recherche Scientifique
37. **Takase K, Mitsushima D, Masuda J, Mogi K, Funabashi T, Endo Y, Kimura F** 2005 Feeding with powdered diet after weaning affects sex difference in acetylcholine release in the hippocampus in rats. Neuroscience 136:593–599
38. **Mitsushima D, Mizuno T, Kimura F** 1996 Age-related changes in diurnal acetylcholine release in the prefrontal cortex of male rats as measured by microdialysis. Neuroscience 72:429–434
39. **Mitsushima D, Yamanoi C, Kimura F** 1998 Restriction of environmental space attenuates locomotor activity and hippocampal acetylcholine release in male rats. Brain Res 805:207–212
40. **Masuda J, Mitsushima D, Funabashi T, Kimura F** 2005 Sex and housing conditions affect the 24-h acetylcholine release profile in the hippocampus in rats. Neuroscience 132:537–542
41. **Mitsushima D, Jinnai K, Kimura F** 1997 Possible role of the γ-aminobutyric acid-A receptor system in the timing of the proestrous luteinizing hormone surge in rats. Endocrinology 138:1944–1948
42. **Murphy BEP** 1967 Some studies of the protein-binding of steroids and their application to the routine micro and ultramicro measurement of various steroids in body fluids by competitive protein-binding radioassay. J Clin Endocrinol Metab 27:973–990
43. **Mitsushima D, Funabashi T, Shinohara K, Kimura F** 2003 Rats living in small cages respond to restraint stress with adrenocortical corticosterone release but not with hippocampal acetylcholine release. Psychoneuroendocrinology 28:574–583
44. **Butcher RL, Collins WE, Fugo NW** 1974 Plasma concentration of LH, FSH, prolactin, progesterone and estradiol-17β throughout the 4-day estrous cycle of the rat. Endocrinology 94:1704–1708
45. **Mitsushima D, Shwe TTW, Funabashi T, Shinohara K, Kimura F** 2002 GABA release in the medial preoptic area of cyclic female rats. Neuroscience 113:109–114
46. **Daniel JM, Dohanichi GP** 2001 Acetylcholine mediates the estrogen-induced increase in NMDA receptor binding in CA1 of the hippocampus and associated improvement in working memory. J Neurosci 21:6949–6956
47. **Lâm TT, Leranth C** 2003 Role of the medial septum diagonal band of Broca cholinergic neurons in oestrogen-induced spine synapse formation on hippocampal CA1 pyramidal cells of female rats. Eur J Neurosci 17:1997–2005
48. **Luine VN, Renner KJ, McEwen BS** 1986 Sex-dependent differences in estrogen regulation of choline acetyltransferase are altered by neonatal treatments. Endocrinology 119:874–878
49. **McEwen BS, Alves SE** 1999 Estrogen actions in the central nervous system. Endocr Rev 20:279–307
50. **Pongrac JL, Gibbs RB, Defranco DB** 2004 Estrogen-mediated regulation of cholinergic expression in basal forebrain neurons requires extracellular signal-regulated kinase activity. Neuroscience 124:809–816
51. **Romeo RD, McCarthy JB, Wang A, Milner TA, McEwen BS** 2005 Sex differences in hippocampal estradiol-induced *N*-methyl-D-aspartic acid binding and ultrastructural localization of estrogen receptor α. Neuroendocrinology 81:391–399
52. **Leranth C, Petnehazy O, MacLusky NJ** 2003 Gonadal hormones affect spine synaptic density in the CA1 hippocampal subfield of male rats. J Neurosci 23: 1588–1592
53. **Gold PE** 2003 Acetylcholine modulation of neural systems involved in learning and memory. Neurobiol Learn Mem 80:194–210
54. **Parent MB, Baxter MG** 2004 Septohippocampal acetylcholine: involved in but not necessary for learning and memory? Learn Mem 11:9–20
55. **Cole AE, Nicoll RA** 1983 Acetylcholine mediates a slow synaptic potential in hippocampal pyramidal cells. Science 221:1299–1301
56. **Markram H, Segal M** 1990 Long-lasting facilitation of excitatory postsynaptic potentials in the rat hippocampus by acetylcholine. J Physiol 427:381–393
57. **Widmer H, Ferrigan L, Davies CH, Cobb SR** 2006 Evoked slow muscarinic acetylcholinergic synaptic potentials in rat hippocampal interneurons. Hippocampus 16:617–628
58. **Kotani S, Yamauchi T, Teramoto T, Ogura H** 2006 Pharmacological evidence of cholinergic involvement in adult hippocampal neurogenesis in rats. Neuroscience 142:505–514
59. **Fornari RV, Moreira KM, Oliveira MG** 2000 Effects of the selective M_1 muscarinic receptor antagonist dicyclomine on emotional memory. Learn Mem 7:287–292
60. **Miyakawa T, Yamada M, Duttaroy A, Wess J** 2001 Hyperactivity and intact hippocampus-dependent learning in mice lacking the M_1 muscarinic acetylcholine receptor. J Neurosci 21:5239–5250
61. **McEwen BS, Lasley EN** 2002 The end of stress as we know it. 1st ed. Washington, DC: National Academies Press
62. **Kudo K, Qiao CX, Kanba S, Arita J** 2004 A selective increase in phosphorylation of cyclic AMP response element-binding protein in hippocampal CA1 region of male, but not female, rats following contextual fear and passive avoidance conditioning. Brain Res 1024:233–243
63. **Edinger KL, Lee B, Frye CA** 2004 Mnemonic effects of testosterone and its 5α-reduced metabolites in the conditioned fear and inhibitory avoidance tasks. Pharmacol Biochem Behav 78:559–568
64. **Morgan MA, Pfaff DW** 2001 Effects of estrogen on activity and fear-related behaviors in mice. Horm Behav 40:472–482
65. **Gupta RR, Sen S, Diepenhorst LL, Rudick CN, Maren S** 2001 Estrogen modulates sexually dimorphic contextual fear conditioning and hippocampal long-term potentiation (LTP) in rats. Brain Res 888:356–365
66. **Jakab RL, Harada N, Naftolin F** 1994 Aromatase- (estrogen synthetase) immunoreactive neurons in the rat septal area. A light and electron microscopic study. Brain Res 664:85–93
67. **Naftolin F, Horvath T, Balthazart J** 2001 Estrogen synthetase (aromatase) immunohistochemistry reveals concordance between avian and rodent limbic systems and hypothalami. Exp Biol Med 226:717–725
68. **Leranth C, Hajszan T, MacLusky NJ** 2004 Androgens increase spine synapse density in the CA1 hippocampal subfield of ovariectomized female rats. J Neurosci 24:495–499
69. **MacLusky NJ, Hajszan T, Leranth C** 2004 Effects of dehydroepiandrosterone and flutamide on hippocampal CA1 spine synapse density in male and female rats: implications for the role of androgens in maintenance of hippocampal structure. Endocrinology 145:4154–4161
70. **Graves FC, Wallen K** 2006 Androgen-induced yawning in rhesus monkey females is reversed with a nonsteroidal anti-androgen. Horm Behav 49:233–236
71. **Bimonte-Nelson HA, Singleton RS, Nelson ME, Eckman CB, Barber J, Scott, TY, Granholm AE** 2003 Testosterone but not nonaromatizable dihydrotestosterone, improves working memory and alters nerve growth factor levels in aged male rats. Exp Neurol 181:301–312
72. **Burnstein KL, Maiorino CA, Dai JL, Cameron DJ** 1995 Androgen and glucocorticoid regulation of androgen receptor cDNA expression. Mol Cell Endocrinol 115:177–186
73. **Larkowski TD, Drengler SM, Tanzer L, Jones KJ** 2000 Androgen receptor mRNA regulation in adult male and female hamster facial motorneurons: effects of axotomy and exogenous androgens. J Neurobiol 45:207–214
74. **Hojo Y, Hattori T, Enami T, Furukawa A, Suzuki K, Ishii H, Mukai H, Morrison JH, Janssen WGM, Kominami S, Harada N, Kimoto T, Kawato S** 2003 Adult male rat hippocampus synthesizes estradiol from pregnenolone by cytochromes P45017α and P450 aromatase localized in neurons. Proc Natl Acad Sci USA 101:865–870
75. **Bingaman EW, Van de Kar LD, Yracheta JM, Li Q, Gray TS** 1995 Castration attenuates prolactin response but potentiates ACTH response to conditioned stress in the rat. Am J Physiol 269:R856–RR863

76. **Handa RJ, Nunley KM, Lorens SA, Louie JP, McGivern RF, Bollnow MR** 1994 Androgen regulation of adrenocorticotropin and corticosterone secretion in the male rat following novelty and foot shock stressors. Physiol Behav 55:117–124
77. **Viau V, Meaney MJ** 1991 Variations in the hypothalamic-pituitary-adrenal response to stress during the estrous cycle in the rat. Endocrinology 129:2503–2511
78. **Burgess LH, Handa RJ** 1992 Chronic estrogen-induced alterations in adrenocorticotropin and corticosterone secretion, and glucocorticoid receptor-mediated functions in female rats. Endocrinology 131:1261–1269
79. **Lunga P, Herbert J** 2004 17β-Oestradiol modulates glucocorticoid, neural and behavioural adaptations to repeated restraint stress in female rats. J Neuroendocrinol 16:776–785
80. **Lund TD, Munson DJ, Haldy ME, Handa RJ** 2004 Androgen inhibits, while oestrogen enhances, restraint-induced activation of neuropeptide neurones in the paraventricular nucleus of the hypothalamus. J Neuroendocrinol 16:272–278
81. **Figueiredo HF, Ulrich-Lai YM, Choi DC, Herman JP** 2007 Estrogen potentiates adrenocortical responses to stress in female rats. Am J Physiol 292:E1173–E1182
82. **McEwen BS, Sapolsky RM** 1995 Stress and cognitive function. Curr Opin Neurobiol 5:205–216
83. **Sapolsky RM, Romero LM, Munck AU** 2000 How do glucocorticoids influence stress responses? Integrating permissive, suppressive, stimulatory, and preparative actions. Endocr Rev 21:55–89
84. **Buchanan TW, Lovallo WR** 2001 Enhanced memory for emotional material following stress-level cortisol treatment in humans. Psychoneuroendocrinology 26: 307–317
85. **Morris R** 2007 Stress and hippocampus. In: Andersen P, Morris R, Amaral D, Bliss T, O'Keefe J, eds. The hippocampus book. New York: Oxford University Press; 751–768
86. **Kovacs GL, Telegdy G, Lissak K** 1977 Dose-dependent action of corticosteroids on brain serotonin content and passive avoidance behavior. Horm Behav 8:155–165
87. **Flood JF, Vidal D, Bennett EL, Orme AE, Vasquez S, Jarvik ME** 1978 Memory facilitating and anti-amnesic effects of corticosteroids. Pharmacol Biochem Behav 8:81–87
88. **Roozendaal B, McGaugh JL** 1996 Amygdaloid nuclei lesions differentially affect glucocorticoid-induced memory enhancement in an inhibitory avoidance task. Neurobiol Learn Mem 65:1–8
89. **Endo Y, Nishimura JI, Kimura F** 1996 Impairment of maze learning in rats following long-term glucocorticoid treatments. Neurosci Lett 203:199–202
90. **Yerkes RM, Dodson JD** 1908 The relation of strength of stimulus to rapidly of habit-formation. J Comp Neurol Psychol 18:459–482
91. **Hesen W, Joëls M** 1993 Modulation of carbachol responsiveness in rat CA1 pyramidal neurons by corticosteroid hormones. Brain Res 627:159–167
92. **Helm KA, Han JS, Gallagher M** 2002 Effects of cholinergic lesions produced by infusions of 192 IgG-saporin on glucocorticoid receptor mRNA expression in hippocampus and medial prefrontal cortex of the rat. Neuroscience 115:765–774
93. **Park E, Chan O, Li Q, Kiraly M, Matthews SG, Vranic M, Riddell MC** 2005 Changes in basal hypothalamo-pituitary-adrenal activity during exercise training are centrally mediated. Am J Physiol 289: R1360–R1371

***Endocrinology* is published monthly by The Endocrine Society (http://www.endo-society.org), the foremost professional society serving the endocrine community.**

Available online at www.sciencedirect.com
ScienceDirect
Neuroscience Letters 432 (2008) 58–63

Estrogen modulates Bcl-2 family protein expression in the sexually dimorphic nucleus of the preoptic area of postnatal rats

Shinji Tsukahara*, Rieko Hojo, Yoshiko Kuroda, Hidekazu Fujimaki

Research Center for Environmental Risk, National Institute for Environmental Studies, Onogawa 16-2, Tsukuba, Ibaraki 305-8506, Japan

Received 2 October 2007; received in revised form 2 December 2007; accepted 4 December 2007

Abstract

In the sexually dimorphic nucleus of the preoptic area (SDN-POA) of postnatal rats, apoptotic cells are detected more frequently in females than males. This sex difference is under the influence of aromatized androgen. We have reported that there are sex differences in the levels of Bcl-2 (female < male) and Bax (female > male) in the central division of the medial preoptic nucleus (MPNc), a significant component of the SDN-POA, followed by a sex difference in induction of apoptosis via caspase-3 activation (female > male). In the present study, we examined effects of estradiol benzoate (EB) on expression of Bcl-2 and Bax in the MPNc. Female rats were subcutaneously injected with EB (25 or 50 μg per head) on postnatal day 5. MPNc and caudate putamen (CP) tissues were obtained from EB-treated female and male rats on postnatal day 6. Protein levels of Bcl-2 and Bax were determined by Western blotting. In the MPNc of female rats, EB at a dose of 50 μg/head but not 25 μg/head significantly increased Bcl-2 protein level and decreased Bax protein level. The levels of Bcl-2 and Bax of female rats treated with 50 μg of EB were comparable to those of male rats. However, the protein levels of Bcl-2 and Bax in the CP did not change with EB treatment. These results suggest that estrogen up-regulates Bcl-2 expression and down-regulates Bax expression in the MPNc of postnatal rats. Effects of estrogen on the Bcl-2 family are presumably responsible for sex difference in postnatal apoptosis of the SDN-POA.

Keywords: Estradiol; Apoptosis; Bcl-2; Bax; Sexually dimorphic nucleus of the preoptic area (SDN-POA)

Morphological sex differences in the central nervous system are well documented. In rats, the sexually dimorphic nucleus of the preoptic area (SDN-POA) of males is larger and has more neurons than that of females [12,13]. The volume of the SDN-POA in male rats decreases when they are neonatally castrated [12]. In contrast, in female rats that receive testosterone propionate (TP) treatments in the perinatal period, the SDN-POA enlarges until it is as large as that of normal males [7,12]. Thus, the gonadal steroidal milieu during the perinatal period is closely related to establishment of sexual dimorphism of the SDN-POA.

Although the mechanisms involved in formation of the sexually dimorphic nuclei are unclear, several lines of evidence indicate that they involve sex differences in the number of neurons killed by apoptosis during brain development. In the central division of the medial preoptic nucleus (MPNc), which is a significant component of the SDN-POA, the number of apoptotic cells is greater in female rats than in male rats in the postnatal period [4,5]. The sex difference in the apoptotic cell number of the MPNc in the postnatal period negatively correlates with the sex difference in the volume and cell number in adulthood. In addition, in neonatally gonadectomized female and male rats, the number of apoptotic cells in the MPNc in the postnatal period is decreased by TP treatment [4,5]. Furthermore, in postnatal female rats, estradiol benzoate (EB) reduces the number of apoptotic cells in the SDN-POA [2]. Together, these findings suggest that estradiol, which is synthesized from testosterone by aromatase in the brain, inhibits apoptotic cell death in the SDN-POA of postnatal rats.

The Bcl-2 family, which is involved in regulation of cell death and survival via the mitochondrial apoptotic pathway, plays an important role in the formation of the sexually dimorphic nuclei [8]. The anteroventral periventricular nucleus (AVPV) of male mice and the spinal nucleus of the bulbocavernosus (SNB) of female mice normally have fewer cells than those of the opposite sex, but overexpression of anti-apoptotic Bcl-2 increases the cell numbers of these nuclei and reduces the sex differences in their cell numbers [24]. In addition, in pro-apoptotic Bax knockout mice, morphological sex differences in the AVPV, SNB, and

* Corresponding author. Tel.: +81 29 850 2705; fax: +81 29 850 2588.
E-mail address: tsukahara@nies.go.jp (S. Tsukahara).

0304-3940/$ – see front matter © 2007 Elsevier Ireland Ltd. All rights reserved.
doi:10.1016/j.neulet.2007.12.006

the principal nucleus of the bed nucleus of the stria terminalis (BSTp) are reduced or absent [9,16].

We previously reported that, in the MPNc of postnatal rats, there are sex differences in the expression levels of Bcl-2 (female < male) and Bax (female > male) and in the number of neurons containing active caspase-3 (female > male) [21]. These findings suggest that, in the SDN-POA of postnatal rats, the sex difference in the number of apoptotic cells is caused by a sex difference in the apoptotic signal cascade that involves Bcl-2, Bax and caspase-3. However, it is unclear whether estradiol modulates this apoptotic signal cascade in the SDN-POA of postnatal rats. In the present study, we investigated the effects of EB on expression of Bcl-2 and Bax in the SDN-POA of postnatal female rats.

Pregnant Long-Evans rats were purchased as breeding stock (Institute for Animal Reproduction, Kasumigaura, Japan), and were bred with a 12-h light/12-h dark cycle at 23 ± 1 °C with free access to water and food. Female and male pups delivered by the breeding stock were used in the present experiments. All experiments were conducted according to the Guidelines for the Care and Use of Experimental Animals of the National Institute of Environmental Studies.

On postnatal day 5 (PD5; day of birth = PD1), female pups were subcutaneously injected with 25 or 50 μg of EB dissolved in 0.05 ml corn oil (EB25 and EB50 groups, respectively), or were subcutaneously injected with the same volume of corn oil (control group). The doses of EB used in the present experiment were set in accordance with a report showing effects of EB on the number of apoptotic cells in sexually dimorphic nuclei of rats [2]. The EB25 and EB50 groups, the control group, and male pups were maintained with maternal care until MPNc tissue samples were obtained from them. On PD6 (18–21 h after EB treatment), in order to obtain the MPNc tissue samples, pups were decapitated, and then the brain was removed. Brain slices at the chiasmatic level were cut at a thickness of 400 μm using a microslicer (Dosaka EM, Kyoto, Japan). Immediately after the brain slices were obtained, tissue fragments of the MPNc were bilaterally isolated using a stainless steel pipe (inner diameter, 0.65 mm) and quickly frozen. The frozen tissues were kept at −80 °C until they were used for Western blotting for Bcl-2 and Bax. In addition, a part of the caudate putamen (CP) was isolated from 400-μm-thick brain slices using a stainless steel pipe (inner diameter, 0.9 mm), and the protein levels of Bcl-2 and Bax in the CP tissue were also examined.

After the MPNc and CP tissues were isolated, the brain slices were fixed with 10% formalin–saline, and stained with NeuroTrace 500/525 green fluorescent Nissl stain solution (Molecular Probes, Inc., Eugene, OR) according to the manufacturer's protocol. The stained slices were observed under a fluorescent microscope to determine the location of the removed tissue.

Isolated tissue fragments were homogenized in lysis buffer (CelLytic; Sigma Chemical Co., St. Louis, MO) containing a protease inhibitor cocktail (1:4000; Sigma). The homogenate was centrifuged at 16,000 × *g* for 30 min at 4 °C. The protein concentration of the supernatant was determined using a QuantiPro BCA assay kit (Sigma), and the supernatant was then mixed with 1/4 volume of 0.29 M Tris–HCl (pH 6.8) containing 8.3% sodium dodecyl sulfate, 25% glycerol, 7.75% dithiothreitol, and 0.01% bromphenol blue. After the samples were heated at 95 °C for 4 min, equal amounts of protein were separated by electrophoresis on 12.5% sodium dodecyl sulfate-polyacrylamide gels ($n = 6$ for control females; $n = 4$ for EB25 and EB50 females; $n = 5$ for males). The proteins were electrophoretically transferred from the gel to a polyvinylidene difluoride membrane.

After transfer, the membranes were rinsed in TBST (20 mM Tris–HCl (pH 7.6), 0.9% NaCl, and 0.1% Tween-20) and blocked with 5% nonfat dry milk in TBST for 1 h at room temperature. After rinsing in TBST, the membranes were incubated overnight at 4 °C in the blocking buffer containing mouse anti-Bcl-2 antibody (1:400; Santa Cruz Biotechnology, Santa Cruz, CA) or rabbit anti-Bax antibody (1:1000; Cell Signaling Technology, Beverly, MA). Membranes were rinsed in TBST, and then were incubated with horseradish peroxidase-conjugated goat anti-mouse IgG (1:10,000; Chemicon International, Temecula, CA) or horseradish peroxidase-conjugated goat anti-rabbit IgG (1:2000; Cell Signaling) in TBST for 1 h at room temperature. After rinsing in TBST, immunoreactive signals were visualized by applying Western lightning chemiluminescence reagent plus (PerkinElmer, Boston, MA) and exposing the membrane to X-ray film. The membranes were then rinsed in TBST, incubated with restore Western blot stripping buffer (Pierce, Rockford, IL) for 30 min at 37 °C, and then subjected to the above-described blotting process but using mouse anti-beta-tubulin antibody (1:2000; NeoMarkers, Fremont, CA) as the primary antibody.

Densitometry of immunoreactive signals was performed using ImageJ 1.31 (National Institutes of Health, Bethesda, MD). The density of signals for Bcl-2 or Bax protein was normalized by dividing it by the density for the beta-tubulin-immunoreactive signal in the same sample, and was expressed as the relative amount of protein (%), with the mean density of the control group set at 100%. Differences among groups in the protein levels of Bcl-2 and Bax were analyzed by one-way analysis of variance. When significant overall effects were detected, Fisher's PLSD test was performed as post hoc analysis. In the post hoc analysis, a probability value of $p < 0.05$ was considered to indicate statistical significance.

In fluorescent microscopy of brain slices after isolation of medial preoptic tissues, it was observed that the MPNc and a part of the medial preoptic nucleus surrounding the MPNc was bilaterally isolated from brain slices at the chiasmatic level (Fig. 1A and B). It was confirmed that all tissue fragments used for experiments contained the MPNc. Tissues of the CP were isolated from brain slices, as shown in Fig. 1C and D.

One-way analysis of variance indicated that there were significant differences in the relative level of Bcl-2 protein (~26 kDa), which was normalized to the level of beta-tubulin (~55 kDa), in the MPNc among groups [$F(3,15) = 8.21$, $p < 0.005$]. The Bcl-2 protein level in the MPNc of EB50 females was significantly higher than that of the control females or EB25 females (Fig. 2A). The Bcl-2 protein level of EB25 females did not significantly differ from that of the control females. There was no significant difference in the Bcl-2 protein level between the EB50 females and normal males, although the control and EB25

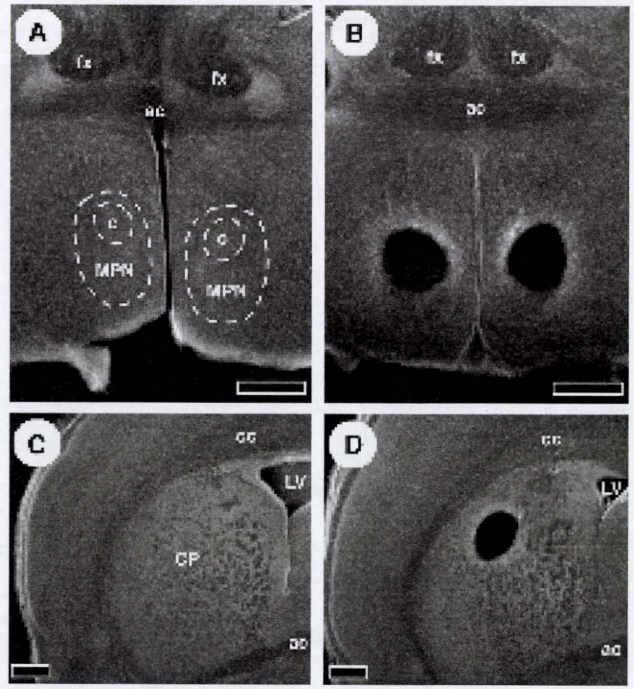

Fig. 1. Photomicrographs of the preoptic area and caudate putamen of fluorescent Nissl-strained brain slices taken from intact PD6 rats (A and C), an MPNc-isolated PD6 rat (B), and a CP-isolated PD6 rat (D). Scale bars indicate 0.5 mm. ac: anterior commissure; c: central division of the MPN; cc: corpus callosum; CP: caudate putamen; fx: fornix; LV: lateral ventricle; MPN: medial preoptic nucleus.

females had a significantly lower level of Bcl-2 protein in the MPNc than normal male rats. In the MPNc, the relative level of Bax protein (~24 kDa) normalized to the level of beta-tubulin was also significantly different among groups [$F(3,15) = 8.44$, $p < 0.005$]. The Bax protein level in the MPNc of EB50 females was significantly less than that of the control females or EB25 females, although the Bax protein level of EB25 females did not significantly differ from that of the control females (Fig. 2B). The Bax protein level of EB50 females was comparable to that of normal males with no significant difference. On the contrary, one-way analysis of variance revealed no significant difference in the levels of Bcl-2 protein [$F(3,15) = 0.71$, $p = 0.561$] and Bax protein [$F(3,15) = 2.08$, $p = 0.147$] of the CP tissue among groups (Fig. 2C and D).

In a histological study of DNA fragmentation as a marker of apoptotic cells, EB treatment on PD5 decreased the number of apoptotic cells in the SDN-POA of female rats 24 h after the EB treatment [2]. In another study, the number of apoptotic cells in the SDN-POA on PD6 was greater for neonatally castrated male rats than for males that were neonatally castrated and were injected with TP on PD5 [5]. These reports indicate that apoptotic cell death in the SDN-POA on PD6 is inhibited when animals are treated with estradiol or testosterone on PD5. Therefore, in the present study, in order to investigate effects of estradiol on expression of Bcl-2 and Bax in the SDN-POA of postnatal rats, female rats were injected with EB on PD5 and sacrificed on PD6.

In the present study, the protein level of Bcl-2 in the MPNc of EB50 females was significantly higher than that of the control females. On the contrary, the protein level of Bax in the MPNc of EB50 females was significantly less than that of the control females. These results indicate that EB treatment at a dose of 50 μg/head stimulates the expression of Bcl-2 and inhibits the expression of Bax in the SDN-POA of postnatal female rats. It has been reported that estradiol up-regulates the expression of Bcl-2 in the hypothalamus of adult rats [10]. In addition, testosterone increases Bcl-2 immunoreactivity in the SNB [25], which is a sexually dimorphic nucleus that is larger in male rats than in female rats [3] and contains androgen-sensitive motoneurons [18]. Other studies have shown that, in the peripheral tissues, the expression of Bax is up- [22] and down-regulated [11] by gonadal steroids. These studies and the present findings suggest

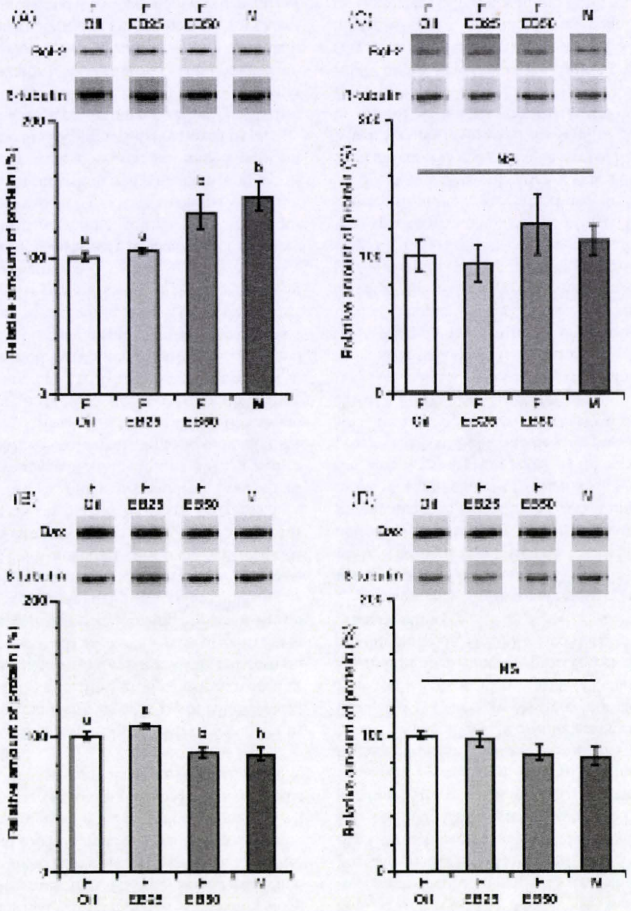

Fig. 2. Effects of estradiol benzoate (EB) on the protein levels of Bcl-2 and Bax in the MPNc (A and B) and CP (C and D) of postnatal rats. Female rats were treated with vehicle oil (Oil), or with 25 or 50 μg of EB (EB25 or EB50) on PD5. The MPNc and CP tissue samples were obtained on PD6. Values (mean ± S.E.M.) with different characters are significantly ($p < 0.05$) different from each other. NS: not significant.

that gonadal steroids, estradiol and testosterone, can change the level of Bcl-2 and Bax expression.

In the mitochondrial control of apoptosis, the Bcl-2 family members modulate caspase-9 activity via regulation of cytochrome *c* release from mitochondria, thereby modulating the downstream activation of caspase-3, an executioner protease of apoptosis [15,19,20]. Neuronal cell death via this apoptotic pathway is implicated in brain development [1,6,17]. Moreover, Bcl-2 and Bax play an essential role in the formation of the sexually dimorphic nuclei. In transgenic mice overexpressing Bcl-2, sex differences in the cell number of the AVPV and SNB are reduced with increase in the cell number of these nuclei [24]. In addition, morphological sex differences in the AVPV, SNB, and BSTp are reduced or absent in Bax knockout mice [9,16]. It was further reported that, in the BSTp of postnatal mice, the sex difference in the number of apoptotic cells (female > male) was completely eliminated by a null mutation of Bax gene [14].

In the MPNc of postnatal rats, we have previously reported that the protein expression levels of Bcl-2 in males and of Bax in females were significantly higher than those in the opposite sex, and that there are sex differences in the number of neurons containing active caspase-3 (female > male) [21]. These findings

suggest that the mitochondrial apoptotic pathway involving Bcl-2 and Bax plays an important role not only in the formation of the AVPV, SNB, and BSTp but also in the formation of the SDN-POA. The present study also suggests that there are sex differences in the expression of Bcl-2 and Bax in the MPNc of postnatal rats, since the levels of Bcl-2 and Bax proteins of control female rats significantly differ from those of male rats. Furthermore, the levels of both Bcl-2 and Bax proteins in the MPNc of EB50 females were comparable to those of male rats with no significant difference in the present study. In the rat SDN-POA in the postnatal period, the number of apoptotic cells is decreased by EB or TP [2,4,5]. Aromatizable androgen active during the perinatal period increases the size of the SDN-POA in adulthood [7,12]. These findings together with our present results suggest that estradiol inhibits apoptotic cell death in the SDN-POA of postnatal rats by up- and down-regulating the expression of Bcl-2 and Bax, respectively. The effects of estradiol on the expression of Bcl-2 and Bax may contribute to the formation of the SDN-POA at least in part, although the mechanisms for the formation of the sexually dimorphic nuclei remain unclear.

In the AVPV of postnatal rats, the number of apoptotic cells is higher in males than females [23]. EB can increase the number of apoptotic cells in the AVPV of female rats [2]. We had previously reported that the AVPV of postnatal rats has sex differences in the levels of Bcl-2 and Bax expression. The protein level of Bcl-2 in the AVPV was higher in PD1 female rats, whereas the level of Bax protein was lower in PD1 female rats [21]. These indicate that sex differences in apoptosis and effects of EB on apoptosis of the AVPV are opposite to those of the SDN-POA. In the present study, we showed that EB increases the level of Bcl-2 and decreases the level of Bax in the MPNc of postnatal rats. Conversely, in the AVPV of postnatal rats, estradiol may down-regulate the expression of Bcl-2 and up-regulate the expression of Bax.

In the present study, EB at a dose of 50 μg/head alters the protein levels of Bcl-2 and Bax in the MPNc of postnatal female rats. However, in the CP, EB did not significantly affect the expression levels of Bcl-2 and Bax. The MPNc is a major component of the SDN-POA, where morphological sex differences are well demonstrated [12,13]. Thus, these results in the present study suggest that significant effects of EB on the expression of Bcl-2 and Bax in the brain of postnatal rats specifically emerge only in the sexually dimorphic nuclei including the SDN-POA.

A previous study has shown that EB decreases the number of apoptotic cells in the SDN-POA, when female rats are treated with EB at a dose of 25 μg/head on PD5 and sacrificed on PD6 [2]. In the present study, EB at a dose of 50 μg/head but not 25 μg/head significantly altered the levels of Bcl-2 and Bax in the MPNc of female rats, indicating that effective dose of EB in the present study is two times larger than that in the previous study. It is largely unclear why the effective dose of EB is different from each other. However, the difference in the effective dose may arise from the difference in strain of animals studied. We used Long-Evans rats in the present study, whereas Wistar rats were used in the previous study.

In conclusion, the present results indicate that estradiol up-regulates the expression of Bcl-2 and down-regulates the expression of Bax in the MPNc of postnatal rats. The effects of estradiol on the expression of the Bcl-2 family members presumably contribute to sex differences in postnatal apoptosis involved in the formation of the SDN-POA.

Acknowledgements

This work was supported in part by Grants-in-Aid for Scientific Research from the Ministry of Education, Science, Culture, and Sports of Japan (17052013, 17780217, 19681006) to S.T.

References

[1] S. Abe-Dohmae, N. Harada, K. Yamada, R. Tanaka, Bcl-2 gene is highly expressed during neurogenesis in the central nervous system, Biochem. Biophys. Res. Commun. 191 (1993) 915–921.
[2] Y. Arai, Y. Sekine, S. Murakami, Estrogen and apoptosis in the developing sexually dimorphic preoptic area in female rats, Neurosci. Res. 25 (1996) 403–407.
[3] S.M. Breedlove, A.P. Arnold, Sexually dimorphic motor nucleus in the rat lumbar spinal cord: response to adult hormone manipulation, absence in androgen-insensitive rats, Brain Res. 225 (1981) 297–307.
[4] W.C. Chung, D.F. Swaab, G.J. De Vries, Apoptosis during sexual differentiation of the bed nucleus of the stria terminalis in the rat brain, J. Neurobiol. 43 (2000) 234–243.
[5] E.C. Davis, P. Popper, R.A. Gorski, The role of apoptosis in sexual differentiation of the rat sexually dimorphic nucleus of the preoptic area, Brain Res. 734 (1996) 10–18.
[6] T.L. Deckwerth, J.L. Elliott, C.M. Knudson, E.M. Johnson Jr., W.D. Snider, S.J. Korsmeyer, Bax is required for neuronal death after trophic factor deprivation and during development, Neuron 17 (1996) 401–411.
[7] K.D. Dohler, A. Coquelin, F. Davis, M. Hines, J.E. Shryne, R.A. Gorski, Pre- and post-natal influence of testosterone propionate and diethylstilbestrol on differentiation of the sexually dimorphic nucleus of the preoptic area in male and female rats, Brain Res. 302 (1984) 291–295.
[8] N.G. Forger, Cell death and sexual differentiation of the nervous system, Neuroscience 138 (2006) 929–938.
[9] N.G. Forger, G.J. Rosen, E.M. Waters, D. Jacob, R.B. Simerly, G.J. de Vries, Deletion of Bax eliminates sex differences in the mouse forebrain, Proc. Natl. Acad. Sci. U.S.A. 101 (2004) 13666–13671.
[10] L.M. Garcia-Segura, P. Cardona-Gomez, F. Naftolin, J.A. Chowen, Estradiol upregulates Bcl-2 expression in adult brain neurons, Neuroreport 9 (1998) 593–597.
[11] S.B. Goodman, K. Kugu, S.H. Chen, S. Preutthipan, K.I. Tilly, J.L. Tilly, A.M. Dharmarajan, Estradiol-mediated suppression of apoptosis in the rabbit corpus luteum is associated with a shift in expression of Bcl-2 family members favoring cellular survival, Biol. Reprod. 59 (1998) 820–827.
[12] R.A. Gorski, J.H. Gordon, J.E. Shryne, A.M. Southam, Evidence for a morphological sex difference within the medial preoptic area of the rat brain, Brain Res. 148 (1978) 333–346.
[13] R.A. Gorski, R.E. Harlan, C.D. Jacobson, J.E. Shryne, A.M. Southam, Evidence for the existence of a sexually dimorphic nucleus in the preoptic area of the rat, J. Comp. Neurol. 193 (1980) 529–539.
[14] T. Gotsiridze, N. Kang, D. Jacob, N.G. Forger, Development of sex differences in the principal nucleus of the bed nucleus of the stria terminalis of mice: role of Bax-dependent cell death, Dev. Neurobiol. 67 (2007) 355–362.
[15] D.R. Green, J.C. Reed, Mitochondria and apoptosis, Science 281 (1998) 1309–1312.
[16] D.A. Jacob, C.L. Bengston, N.G. Forger, Effects of Bax gene deletion on muscle and motoneuron degeneration in a sexually dimorphic neuromuscular system, J. Neurosci. 25 (2005) 5638–5644.

[17] K. Kuida, T.S. Zheng, S. Na, C. Kuan, D. Yang, H. Karasuyama, P. Rakic, R.A. Flavell, Decreased apoptosis in the brain and premature lethality in CPP32-deficient mice, Nature 384 (1996) 368–372.
[18] A. Matsumoto, Y. Arai, G.S. Prins, Androgenic regulation of androgen receptor immunoreactivity in motoneurons of the spinal nucleus of the bulbocavernosus of male rats, J. Neuroendocrinol. 8 (1996) 553–559.
[19] D.E. Merry, S.J. Korsmeyer, Bcl-2 gene family in the nervous system, Annu. Rev. Neurosci. 20 (1997) 245–267.
[20] B. Pettmann, C.E. Henderson, Neuronal cell death, Neuron 20 (1998) 633–647.
[21] S. Tsukahara, M. Kakeyama, Y. Toyofuku, Sex differences in the level of Bcl-2 family proteins and caspase-3 activation in the sexually dimorphic nuclei of the preoptic area in postnatal rats, J. Neurobiol. 66 (2006) 1411–1419.
[22] B. Xie, S.W. Tsao, Y.C. Wong, Sex hormone-induced mammary carcinogenesis in the female Noble rats: expression of Bcl-2 and Bax in hormonal mammary carcinogenesis, Breast Cancer Res. Treat. 61 (2000) 45–57.
[23] M. Yoshida, K. Yuri, Z. Kizaki, T. Sawada, M. Kawata, The distributions of apoptotic cells in the medial preoptic areas of male and female neonatal rats, Neurosci. Res. 36 (2000) 1–7.
[24] S.L. Zup, H. Carrier, E.M. Waters, A. Tabor, L. Bengston, G.J. Rosen, R.B. Simerly, N.G. Forger, Overexpression of Bcl-2 reduces sex differences in neuron number in the brain and spinal cord, J. Neurosci. 23 (2003) 2357–2362.
[25] S.L. Zup, N.G. Forger, Testosterone regulates Bcl-2 immunoreactivity in a sexually dimorphic motor pool of adult rats, Brain Res. 950 (2002) 312–316.

Synaptic activity-responsive element in the *Arc/Arg3.1* promoter essential for synapse-to-nucleus signaling in activated neurons

Takashi Kawashima[a,1], Hiroyuki Okuno[a,1,2], Mio Nonaka[a], Aki Adachi-Morishima[a], Nan Kyo[a], Michiko Okamura[a], Sayaka Takemoto-Kimura[a], Paul F. Worley[b], and Haruhiko Bito[a,c,2]

[a]Department of Neurochemistry, Graduate School of Medicine, University of Tokyo, Bunkyo-ku, Tokyo 113-0033, Japan; [c]CREST-JST, Kawaguchi, Saitama 332-0012, Japan; and [b]Department of Neuroscience, Johns Hopkins University School of Medicine, Baltimore, MD 21205

Edited by Yoshito Kaziro, Kyoto University, Kyoto, Japan, and approved November 17, 2008 (received for review July 14, 2008)

The neuronal immediate early gene *Arc/Arg-3.1* is widely used as one of the most reliable molecular markers for intense synaptic activity in vivo. However, the *cis*-acting elements responsible for such stringent activity dependence have not been firmly identified. Here we combined luciferase reporter assays in cultured cortical neurons and comparative genome mapping to identify the critical synaptic activity-responsive elements (SARE) of the *Arc/Arg-3.1* gene. A major SARE was found as a unique ≈100-bp element located at >5 kb upstream of the *Arc/Arg-3.1* transcription initiation site in the mouse genome. This single element, when positioned immediately upstream of a minimal promoter, was necessary and sufficient to replicate crucial properties of endogenous *Arc/Arg-3.1*'s transcriptional regulation, including rapid onset of transcription triggered by synaptic activity and low basal expression during synaptic inactivity. We identified the major determinants of SARE as a unique cluster of neuronal activity-dependent *cis*-regulatory elements consisting of closely localized binding sites for CREB, MEF2, and SRF. Consistently, a SARE reporter could readily trace and mark an ensemble of cells that have experienced intense activity in the recent past in vivo. Taken together, our work uncovers a novel transcriptional mechanism by which a critical 100-bp element, SARE, mediates a predominant component of the synapse-to-nucleus signaling in ensembles of Arc/Arg-3.1-positive activated neurons.

immediate-early genes | MEF2 | SRF | calcium | CREB

Fine tuning of gene expression and protein translation in mature neurons is of vital importance to brain function (1). Aberrance of adaptive responses such as long-term memory or late-phase synaptic plasticity has indeed been the hallmark of several genetically engineered mouse mutants in which the expression or the function of key transcription factors have been altered (2, 3). Thus it appears that the supply of neuronal proteins must be tightly matched to the cellular demand at any given time, to maintain proper neuronal circuit function.

One critical determinant of neuronal gene expression is the neuron's own activity. Dramatic changes in gene expression have been reported upon robust reorganization of sensory information processing (such as during critical period plasticity of the visual cortex), or through characteristic cognitive processes (such as establishment of long-term memory) (4–6). Barrages of synaptic activity that alters synaptic strength can directly up- or downregulate various constituents of the synaptic machinery and many signaling molecules (7–9). Studies of the transcriptional activation mechanisms leading to upregulation of the immediate early genes c-*fos*, *zif*268, and of the brain-derived neurotrophic factor (BDNF) indicated that transcription factors such as the Ca^{2+}/cAMP-response element binding protein (CREB) and the serum response factor (SRF) may play a privileged role as key neuronal activity sensors in the nucleus (10–12).

An activity-regulated cytoskeleton-associated protein (Arc/Arg-3.1) has recently emerged as an attractive candidate effector molecule/immediate early gene product (13, 14), whose induction may correlate, at least in part, with the induced synaptic alteration phenotype (15–18). Furthermore, *Arc/Arg-3.1* transcription is induced extremely rapidly and *Arc/Arg-3.1* mRNA detection, by fluorescence in situ hybridization, has now been validated as a reliable trace of intense synaptic activity within a neuronal ensemble in the hippocampus (e.g., during novelty exposure), in the amygdala (e.g., during acquisition of long-term fear memory), or in the sensory cortices (e.g., after intense sensory experience following sensory deprivation) (19–22). Despite the growing interest in Arc/Arg-3.1 function, however, surprisingly little is yet known about the genomic mechanism by which acute delivery of synaptic information can be reliably encoded into *Arc/Arg-3.1* transcriptional events in the nucleus. To address this question, we investigated the *cis*-acting enhancer elements responsible for such stringent neuronal activity dependence.

Results

Presence of a Strong Synaptic Activity-Responsive Element in a Distal Portion of the Mouse *Arc/Arg-3.1* Promoter. We performed transcriptional reporter assays using primary culture neurons in which endogenous *Arc/Arg-3.1* is rapidly and transiently induced by 4AP/BIC stimulation (Fig. 1*A*). In the mouse genome, 7 conserved regions exceeding 65% identity per 100 bp with humans were found between 0 and −5 kb (from the transcription initiation site), and 1 distal region was mapped between −6 kb and −7 kb (Fig. 1*B*). No further conserved regions were found between −7 kb and −10 kb.

Prior studies have demonstrated the role of a proximal region (<2 kb) of the *Arc/Arg-3.1* promoter in its activity dependence (23, 24). Consistent with this, proximal regions [Arc1000 (−996 to +198) and Arc2000 (−1996 to +198)] showed 2- to 3-fold induction after stimulation in our assays (Fig. 1*C*). Genomic regions up to 3 kb (Arc3000, −2996 to +198) conferred an 8-fold induction (Fig. 1*C*). The activated levels of 4-kb and 5-kb fragments [Arc4000 (−3996 to +198) and Arc5000 (−4996 to +198)] were similar to that of Arc3000, but their basal levels in TTX were significantly lower than those of Arc1000, Arc2000, and Arc3000 ($P < 0.01$), resulting in an ≈20-fold induction (Fig. 1*C*). Unexpectedly, extension of the genomic sequence up to 7 kb (Arc7000, −7065 to +198) resulted in further increase in its induction ability, of >150-fold, in

Author contributions: H.O. and H.B. designed research; T.K., H.O., M.N., and N.K. performed research; A.A.-M., M.O., S.T.-K., and P.F.W. contributed new reagents/analytic tools; T.K., H.O., M.N., N.K., and H.B. analyzed data; and T.K., H.O., M.N., and H.B. wrote the paper.

The authors declare no conflict of interest.

This article is a PNAS Direct Submission.

[1]T.K. and H.O. contributed equally to this work.

[2]To whom correspondence may be addressed. E-mail: hbito@m.u-tokyo.ac.jp or okuno@m.u-tokyo.ac.jp.

This article contains supporting information online at www.pnas.org/cgi/content/full/0806518106/DCSupplemental.

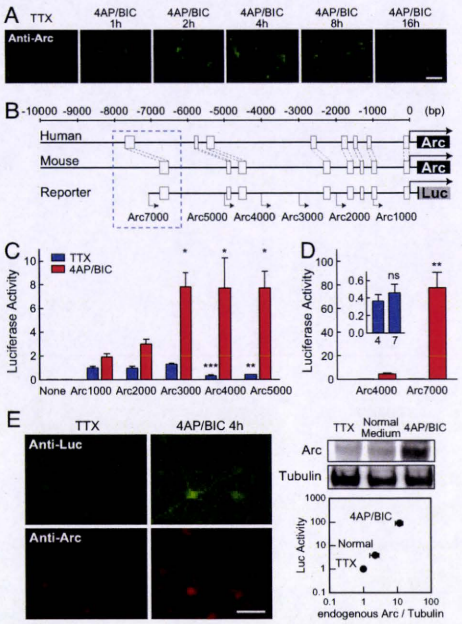

Fig. 1. Multiple regulatory elements in the mouse *Arc/Arg-3.1* promoter. (*A*) Time course of endogenous Arc/Arg-3.1 protein induction by 4AP/BIC stimulation. Cultured cortical neurons pretreated with TTX were stimulated with 4AP/BIC for indicated hours. (Scale bar, 100 μm.) (*B*) Evolutionarily conserved genomic regions in the upstream of the *Arc/Arg-3.1* gene. Regions conserved between mice and humans are shown as white boxes. A destabilized luciferase (Luc-PEST) gene was used as a reporter. (*C*) Transcriptional regulatory activities of Arc1000–5000. Cultured cortical neurons were stimulated with 4AP/BIC for 4 h. Luciferase activities are normalized relative to the activity of Arc1000 under the TTX treatment. This normalization applies to all luciferase assay data in this study. Statistical analyses were performed separately for the TTX and 4AP/BIC data sets. $n = 5$ independent experiments. *, $P < 0.05$; **, $P < 0.01$; ***, $P < 0.001$ compared with the TTX or the 4AP/BIC value of Arc1000 (1-way ANOVA with Tukey's test). (*D*) Strong activation ability of Arc7000. The *y* axis for the basal levels were expanded and shown in the inset for clarity. $n = 7$ independent experiments. **, $P < 0.01$; ns, not significant (paired *t* test) compared with the 4AP/BIC or the TTX value of Arc4000. (*E*) Arc7000-driven luciferase correlates with endogenous Arc induction. *Left*, coexpression of luciferase and endogenous Arc protein after stimulation. (Scale bar, 50 μm.) *Right*, simultaneous quantification of luciferase activities and endogenous Arc protein levels in the same samples. Cell lysates were prepared from neurons with no treatment (normal medium), with TTX, or with 4AP/BIC for 4 h. Arc protein levels were quantified by Western blotting and plotted against the reporter luciferase activities. Duplicated samples were analyzed and shown.

response to stimulation ($P < 0.01$) (Fig. 1*D*), indicating the presence of a very potent enhancer in the most distal conserved region.

We also examined the relative potency of Arc7000 at single-cell resolution, using a destabilized GFP as a fluorescent reporter. As expected from the results of luciferase assays, GFP signals in individual neurons were more elevated downstream of Arc7000 than of Arc4000 ($P < 0.001$) [supporting information (*SI*) Fig. S1]. Additionally, no GFP signals were detected in glial cells (data not shown), indicating that Arc7000 may also determine the neuron-specific expression pattern of the *Arc/Arg-3.1* gene.

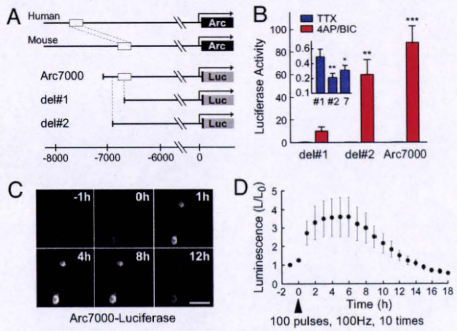

Fig. 2. The distal conserved region is crucial for the Arc7000 promoter activity. (*A*) Arc7000 deletion mutants. The genomic locus framed by a dashed box in Fig. 1 *B* is expanded and shown. (*B*) Presence of a potent enhancer element between Arc7000-del no. 1 and Arc7000-del no. 2. $n = 6$ independent experiments. *, $P < 0.05$; **, $P < 0.01$; ***, $P < 0.001$, compared with the TTX or the 4AP/BIC value of Arc7000-del no. 1 (1-way ANOVA with Tukey's test). (*C* and *D*) Rapid and transient induction of luciferase luminescence by Arc7000 after high-frequency electrical stimulation. Hippocampal neurons transfected with a click beetle luciferase (ELuc) vector was electrically stimulated at 0 h (triangle), and luminescence in the soma was monitored. Representative images were shown in *C*. $n = 9$ neurons. (Scale bar, 50 μm.)

The Arc7000 activity correlated well with the endogenous *Arc/Arg-3.1* expression, because the reporter luciferase after stimulation was mostly coexpressed in the same cells as endogenously induced Arc/Arg-3.1 (Fig. 1*E*), and Western blots showed a linear relation between luciferase activity and endogenous Arc protein levels (Fig. 1*E*).

Identification of a Synaptic Activity-Responsive Element (SARE) in Arc7000 That Is Critical for Activity-Regulated Gene Expression. To pin down the critical enhancer element, we next examined a genomic deletion (del) mutant Arc7000-del no. 1 (−6667 to +198), in which the most distal conserved region was truncated (Fig. 2*A*). This mutant revealed a striking decrease in activity dependence compared with Arc7000 ($P < 0.01$) (Fig. 2*B*). In contrast, Arc7000-del no. 2 (−6893 to +198), in which the conserved region was spared, possessed an activity dependence indistinguishable from Arc7000 (Fig. 2 *A* and *B*). Intriguingly, the basal level of Arc7000-del no. 2 in TTX was indistinguishable from that of Arc7000, but was significantly lower than that of Arc7000-del no. 1 ($P < 0.05$) (Fig. 2*B*).

We then tested whether robust high-frequency synaptic activity triggered by electrical stimulation could induce reporter gene expression downstream of Arc7000 in single neurons. Hippocampal neurons transfected with an Arc7000-ELuc-PEST plasmid were stimulated with field electrical pulses. In responding neurons, luminescence started to increase immediately after the stimulation, reached plateau after 4–6 h, and attenuated gradually after 8 h (Fig. 2 *C* and *D*). This activation time course closely resembled the induction time course of endogenous *Arc/Arg-3.1* following electrical stimulation in vivo (25).

These findings were most consistent with the presence of a potent enhancer, which we termed SARE, in a region between Arc7000-del no. 1 and Arc7000-del no. 2 (Fig. 2 *A* and *B*). Close examination of the evolutionarily conserved region present in del no. 2 but truncated in del no. 1 revealed a series of short conserved sequence stretches, of ≈100 bp (Fig. 3*A*).

To directly test the role of these sequence stretches, we fused a 104-bp fragment (−6793 to −6690) to a TATA-containing short

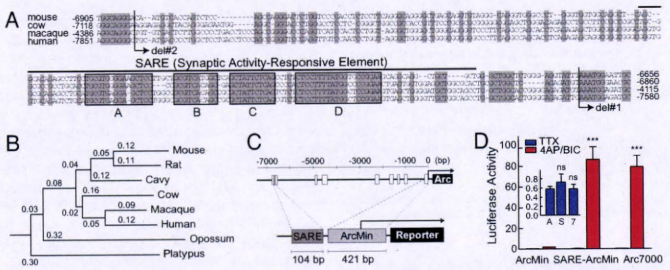

Fig. 3. *Arc/Arg-3.1* SARE replicates Arc7000 promoter activity. (*A*) Comparison across multiple mammalian species. Conserved sequences were highlighted in gray. A short stretch of sequences (thick line) consisted of 4 highly conserved boxes (boxes *A*–*D*) was termed a synaptic activity responsive element (SARE). (*B*) Dendrogram showing the divergence of SARE sequences across various mammalian species. The numbers represent the branch length, which indicates the degree of nucleotide differences. Detailed nucleotide information for this analysis is shown in Fig. S3. (*C*) SARE-ArcMin reporter vector. SARE was fused directly upstream of ArcMin, a TATA-containing sequence around the transcription initiation site of the *Arc/Arg-3.1* gene. (*D*) SARE-ArcMin replicates the activation ability of Arc7000. $n = 5$ independent experiments. ***, $P < 0.001$; ns, not significant, compared with the TTX or the 4AP/BIC value of ArcMin (1-way ANOVA with Tukey's test).

promoter (−222 to +198) of the *Arc/Arg-3.1* gene (SARE-ArcMin) (Fig. 3 *A* and *C*). Luciferase activity driven by SARE-ArcMin was increased >100-fold in response to stimulation (Fig. 3*D*). The basal levels did not differ between SARE-ArcMin and ArcMin (Fig. 3*D*). Importantly, the activation level of SARE-ArcMin was indistinguishable from that of Arc7000 (Fig. 3*D*). The fluorescent protein reporter assay also revealed a dramatic increase in GFP signal positivity in SARE-ArcMin reporter-transfected neurons, following synaptic stimulation in individual cells (Fig. S2). None of the other conserved genomic regions showed such strong enhancer activities on their own (data not shown).

Taken together, these results indicate the existence of a novel SARE in the distal *Arc/Arg-3.1* promoter, which appeared to be critical for replicating the amplitude of activity-induced transcriptional response of the full promoter in the absence of any other adjacent genomic regions, when placed immediately upstream of the minimal *Arc/Arg-3.1* promoter.

Contribution of 3 Activity-Regulated Transcription Factors, CREB, MEF2, and SRF, in SARE Activation. SARE contained 4 conserved sequence stretches (Fig. 3*A*). This raised the possibility that perhaps distinct transcription factors could in principle bind to SARE, and thus, these putative binding sites were tentatively called boxes *A*–*D* (Fig. 3*A*). All 4 boxes were conserved in most mammals, except some species such as the opossum and the platypus (Fig. 3*B* and Fig. S3). To address their requirements, we introduced mutations in each of these boxes, and tested them either in the upstream of a TATA-containing minimal CMV promoter (minCMV, which has virtually no transcriptional activity per se), or in the context of the full Arc7000 promoter (Fig. 4 *A* and *B*). Luciferase activity of SARE-minCMV was increased >80-fold in response to stimulation, and this induction was dramatically diminished by single mutations in boxes *B*, *C*, and *D* ($P < 0.001$). In contrast, a mutation in box *A* had no significant effect (Fig. 4*A*). Combined mutations in both boxes *B* and *D* almost completely blocked the induction (Fig. 4*A*). Similar results were obtained in the context of the full Arc7000 promoter (Fig. 4*B*). These data suggested that boxes *B*, *C*, and *D* were required for the enhancer activity of SARE, and some cooperativity might exist between them. Additionally, the basal level of SARE-minCMV was significantly elevated by mutating box *D* ($P < 0.001$) (Fig. 4*A*), indicating that box *D* might also contribute to attenuating transcription during synaptic inactivity.

We next sought to identify the transcription factors that bound to these sites. Box *B* contained a sequence matching a half site of the consensus binding sequence for CREB (Fig. 4*C*). Box *C* matched the consensus for myocyte enhancer factor 2 (MEF2) with the exception of 2 nucleotides (Fig. 4*C*). The 5′-end of box *D* perfectly matched the consensus for SRF, while the 3′-end perfectly matched the consensus for the ternary complex factors (TCFs), the well-characterized accessory proteins of SRF (Fig. 4*C*). An electrophoretic mobility-shift assay (EMSA) revealed the formation of each specific protein-DNA complex for boxes *B*, *C*, and *D* in nuclear extracts obtained from electroconvulsive shock-treated rat cortices (Fig. 4*C*). Consistent with the consensus sequence matches, each complex was disrupted by adding excess amounts of competitor DNA, and gel supershifts were detected using CREB-, MEF2-, and SRF-specific antibodies. Furthermore, chromatin immunoprecipitation (ChIP) assay using neuronal culture confirmed physical binding of CREB, MEF2, and SRF to SARE in cultured neurons (Fig. 4*D* and Fig. S4). Together, these data strongly suggest that CREB, MEF2, and SRF play critical roles in SARE activation via binding to boxes *B*, *C*, and *D*, respectively (Fig. 4*C*).

We further investigated the intracellular signaling pathways upstream of these transcription factors. The SARE activation in the context of Arc7000 by 4AP/BIC treatment was almost completely suppressed when both AMPA-R and NMDA-R were blocked, confirming that excitatory synaptic inputs trigger the activation (Fig. S5*A*). In addition, the activation was reduced 80% when only NMDA-R was blocked, indicating that synaptic Ca^{2+} influx through NMDA-R is critical for the SARE activation (Fig. S5*A*). The activation was also significantly diminished by KN-93, a Ca^{2+}/calmodulin-dependent protein kinase (CaMK) inhibitor, and U0126, a mitogen-activated protein kinase kinase (MEK) inhibitor (Fig. S5*B*). An essentially similar pharmacological profile was obtained when the SARE activity was tested in the upstream of the minimal CMV promoter (Fig. S5*C*). These results confirmed that SARE was crucial for a large part of the transcriptional response of the *Arc/Arg-3.1* gene that lied downstream of activity-regulated signaling mechanisms, such as CaMK and MAPK cascades, both of which were previously shown to underlie many aspects of neuronal adaptive responses (8, 26).

Visualization of Activated Cells in a Neuronal Circuit Using a SARE Reporter Lentivirus Vector. One potential caveat of the above experiments was that these in vitro assays did not involve genomic integration of the reporter genes. Therefore, we designed a lentivirus-based gene delivery system to introduce SARE-driven reporters into the neuronal genome (Fig. 5). We constructed a lentivirus vector containing 2 expression cassettes placed in opposite directions and separated by an insulator sequence. In 1 cassette,

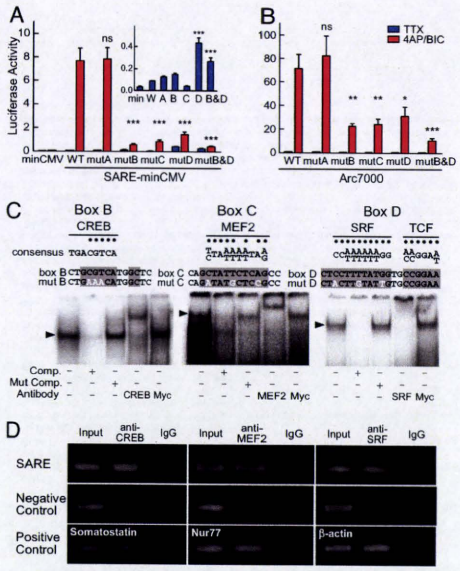

Fig. 4. Involvement of coclustered CREB, MEF2, and SRF in the SARE activation. (*A*) Loss of the SARE activity by mutations in the boxes *B*, *C*, and *D*, but not *A*, in the context of a minimal CMV promoter (SARE-minCMV). Note that the basal level (TTX) was elevated by a mutation in the box *D* (inset). WT, wild-type; ***, $P < 0.001$; ns, not significant, compared with the TTX or the 4AP/BIC value of WT (1-way ANOVA with Tukey's test). (*B*) Loss of the Arc7000 activity by mutations in the boxes *B*, *C*, and *D*. WT, wild-type; *, $P < 0.05$; **, $P < 0.01$; ***, $P < 0.001$; ns, not significant, compared with the 4AP/BIC value of WT (1-way ANOVA with Tukey's test). (*C*) EMSA revealed binding of CREB, MEF2, and SRF to the boxes *B*, *C*, and *D*. *Top*, the matched nucleotides are indicated by dots. The evolutionarily conserved nucleotides are highlighted in gray. The mutated nucleotides are shown with white letters. *Bottom*, representative results of EMSA. The brain nuclear extracts were added with probes of the boxes *B*, *C*, and *D*. Specific DNA-protein complexes (arrows) were observed, which disappeared by adding excessive amounts of unlabeled competitors (Comp), but not by mutated competitors (Mut Comp). Antibodies against CREB, MEF2, and SRF disrupted or supershifted the complexes, whereas a control antibody (anti-Myc) had no effects. (*D*) Chromatin immunoprecipitation (ChIP) assays revealed physical binding of CREB, MEF2, and SRF to SARE in the genome. Target genomic sequences were amplified with specific primer sets by qPCR. *Left*, the genomic region adjacent to the SARE sequence (within 200 bp) was detected in the immunoprecipitates obtained using an anti-CREB antibody, while a negative control sequence 10 kb downstream of SARE was not. The Somatostatin promoter was used as a positive control. *Middle*, detection of SARE in the immunoprecipitates obtained using an anti-MEF2 antibody. The Nur77 promoter was used as a positive control. *Right*, detection of SARE in the immunoprecipitates obtained using an anti-SRF antibody. The β-actin promoter was used as a positive control.

an RFP marker (TurboFP635) was driven under the control of a constitutive *pgk* promoter, while in the other, a d2EGFP reporter was expressed under the control of SARE-ArcMin. A control virus vector contained all these elements except for SARE (Fig. 5*A*).

BDNF is known to effectively induce endogenous Arc/Arg-3.1 expression in neurons. When SARE-ArcMin lentivirus-infected neurons were stimulated with BDNF, GFP signals became detectable in individual neurons (Fig. 5*B*). We further examined, by time-lapse live-cell fluorescence imaging, the activation time course of the genome-integrated SARE, upon high-frequency electrical

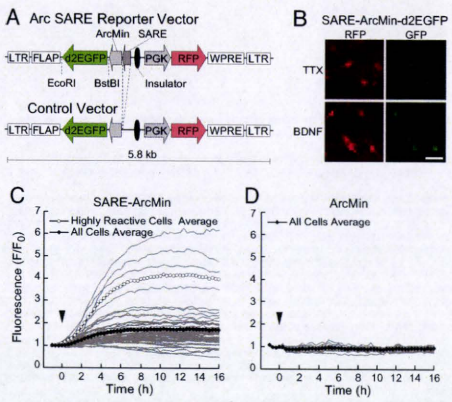

Fig. 5. Lentivirus-based genomic integration of the SARE reporter. (*A*) Design of lentiviral vectors. *Top*, the SARE reporter vector encodes an inducible reporter GFP (d2EGFP) under the control of SARE-ArcMin and a constitutively expressed infection marker RFP (TurboFP635) under the control of a *pgk* promoter. *Bottom*, a control vector lacking SARE. (*B*) Hippocampal neurons infected with the SARE reporter lentivirus were stimulated with BDNF for 6 h at 14 days postinfection. (Scale bar, 50 μm.) (*C*) GFP live-cell imaging of SARE-virus-infected neurons stimulated with high-frequency electrical pulses. Hippocampal neurons infected with the SARE reporter lentivirus were stimulated with field electrical pulses at time 0 h (triangle, 100 pulses at 100 Hz, 9 times), and GFP fluorescence was monitored. Gray lines, traces of individual neurons. Filled squares, the average trace of all neurons examined ($n = 59$). Open circles, the average trace of highly reactive neurons (top 10% of all neurons sorted by the F/F_0 value at the time of 8 h, $n = 6$). (*D*) No GFP fluorescence changes were observed in control-virus-infected neurons. Filled squares, the average trace of all neurons examined ($n = 18$).

stimulation (9 bursts of 100 Hz, 1 sec applied by field stimulation). In most of the SARE-ArcMin lentivirus-infected neurons, GFP fluorescence consistently increased immediately after the stimulation and started to saturate at ≈6–8 h (Fig. 5*C*), while the control virus-infected neurons showed virtually no GFP responses (Fig. 5*D*). Some of the neurons were particularly responsive (Fig. 5*C*), indicative of high copy number expression from multiple and/or transcriptionally favorable genomic loci. Alternatively, these neurons might have been favored because of their highly excitable properties within the neuronal network in culture as previously reported (10).

The above results suggested that the SARE-ArcMin lentivirus might provide a way to visualize specific sets of activated neurons in a given neural circuit in the brain. As a model, we designed an in vivo SARE-ArcMin reporter assay by directly injecting into mouse brains a d2EGFP reporter lentivirus. Consistent with prior reports (27), viral injection into the lateral ventricles of E15 mouse embryos reproducibly resulted in selective integration of infected neurons into layers 2/3 throughout the neocortex, as identified by RFP fluorescence and morphological criteria. No systematic differences were observed in the numbers of infected neurons between the 2 hemispheres. In our conditions, the infection rate was ranging 2–5% of the total cells in layers 2/3.

Cortical activity in the primary visual cortex (V1) was then stimulated by direct manipulation of the visual sensory inputs. Virus-infected mice (3–4 week-old) were sensory-deprived on 1 eye by suture, dark-reared for 1–3 days, and the intact open eye was exposed to light (Fig. 6*A*). Such sensory manipulation produced unilateral activation of the V1, as visualized by high immunoreactivities of endogenous Arc/Arg-3.1 at layers 2/3 and 4 in the

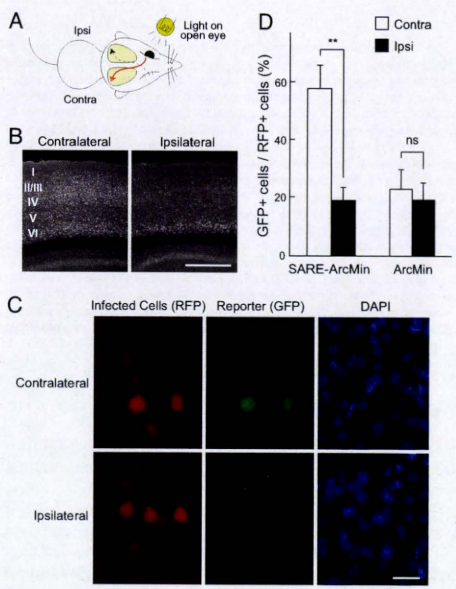

Fig. 6. Visualization of activated neurons in vivo by the SARE viral vector. (*A*) Manipulation of neuronal activity in the mouse visual cortex. The virus-infected mice were sensory-deprived on 1 eye by suture, dark reared for 2–3 days, and exposed to light on the intact open eye. (*B*) Endogenous Arc/Arg-3.1 immunohistochemistry showing unilateral activation of the visual cortex. (Scale bar, 0.5 mm.) (*C*) The SARE reporter virus-infected neurons in layers 2/3 of the visual cortex. Activity-reporter GFP signals were detected in the contralateral side, but not in the ipsilateral side. (Scale bar, 20 μm.) (*D*) The percentages of GFP-positive neurons over RFP-positive neurons in each hemisphere. $n = 6$ mice for SARE-ArcMin, $n = 5$ mice for ArcMin. **, $P < 0.01$; ns, not significant, compared to the ipsilateral side (paired *t* test).

contralateral, but not in the ipsilateral, visual cortex (Fig. 6*B*) (21). Consistent with this pattern, we found that the majority (58.3 ± 7.9%) of RFP-positive neurons were GFP-positive in the contralateral hemisphere that received visual inputs, whereas only a small number (19.3 ± 4.4%) of neurons were positive in the ipsilateral hemisphere (Fig. 6 *C* and *D*). The percentage of GFP- and RFP-double positive neurons in the contralateral hemisphere were comparable with that of Arc/Arg-3.1- and RFP-double positive neurons (57.8 ± 4.6%) (Fig. S6), consistent with coexpression of reporter GFP and endogenous Arc/Arg-3.1. The control ArcMin virus-infected neurons showed low GFP positivity (about 20%) and did not show imbalances between hemispheres (Fig. 6*D*). Taken together, these results indicate that SARE-ArcMin lentivirus could reliably mark activated neurons within a targeted neuronal circuit.

Discussion

Elucidation of a Novel Transcriptional Switch Mechanism That Links Synaptic Activity with Nuclear Transcription: Participation of 3 Major Activity-Regulated Transcription Factors CREB, SRF, and MEF2 in *Arc/Arg-3.1* Transcriptional Response. Our work indicates that the Arc7000 promoter essentially replicates the transcriptional profile of endogenous *Arc/Arg-3.1*, and that a relatively short DNA sequence of ≈100 bp provides a key regulatory mechanism for synapse-to-nucleus signaling. This novel *cis*-acting element contains binding sites for 3 major activity-dependent transcription factors, CREB, MEF2, and SRF, and drove as much reporter induction as Arc7000, in response to synaptic stimuli, when placed upstream of the *Arc/Arg-3.1* minimal promoter. Mutations in either one of the binding sequences resulted in a severe block of transcriptional activity. Thus, intact promoter occupancy by all 3 factors appears to be essential for proper transcriptional activation upon synaptic activity. Pharmacological analyses revealed that synaptic Ca^{2+} influx through NMDA-R was critical for its activation. On the basis of these findings, we named this main activity-sensor for *Arc/Arg-3.1* transcription "synaptic activity-responsive element (SARE)."

A functional CRE is present on many activity-regulated neuronal genes, and CREB has repeatedly been demonstrated to be a critical factor in establishment of long-term plasticity and long-term memory (1, 2, 20). Similarly, a critical role for SRE and SRF in activity-dependent gene expression has extensively been documented (3). Recent evidence also supports a role for MEF2 upstream of various activity-induced genes which directly regulate synaptic functions (28). However, the discovery of a physical clustering, corequirement and sufficiency of the 3 activity-dependent *cis*-regulatory elements located in such close proximity (≈100 bp) in SARE is particularly striking, suggesting that SARE may have a unique role as a coincidence detector for the 3 activity-dependent transcription factors. Intriguingly, we observed that mutations in the SRF-binding site not only abolished SARE activation, but also significantly augmented basal activity under silenced conditions, suggesting an additional role of SRF for transcriptional repression as previously reported in certain contexts in nonneuronal cells (29).

Although distally located SARE likely acts as a major element for activity-dependent *Arc/Arg-3.1* induction, other proximal elements may further cooperate with SARE. Our own data suggested that a proximal region possessed a 2- to 3-fold transcriptional activation ability, consistent with a previous study that showed the contribution of cAMP/MAPK pathways in the activity-dependent response mediated by this region (23). Furthermore, *Egr-1/3* may also mediate the late, protein-synthesis dependent phase of *Arc/Arg-3.1* induction via binding to this proximal region (24).

Mapping of Active Ensembles Within a Neuronal Circuit Can Be Achieved Using SARE-Based Reporters. Detailed analyses of *Arc/Arg-3.1* expression using in situ hybridization have revealed that *Arc/Arg-3.1* transcription is specifically triggered by task- or sensory input-related information processing in several brain areas, including the hippocampus, amygdala, and cerebral cortex (19–21). The shortness of SARE sequence allows designing a virus-based tool to monitor *Arc/Arg-3.1* expression for both in vitro and in vivo imaging. We here performed an experiment where we injected a SARE-reporter lentivirus into embryonic mouse cerebral ventricles in utero, at embryonic day 15 (E15). Prior work established that only the neuronal progenitor cells, present in the ventricular zone (VZ) on the day of injection, are susceptible to viral infection. VZ cells at E15 are destined to become layers 2/3 neurons in the cerebral cortex (27). More than 20 days after lentiviral infection, when the viral integration into the genome has been completed, we quantified the extent of visual activation in layers 2/3 of the primary visual cortex. The virus-injected mice were first dark reared for more than 24 h, which suppressed the reporter expression to the baseline. Following light exposure to 1 eye for 2–3 h, we found that ≈60% of the infected neurons of layers 2/3 were GFP reporter positive, which is consistent with prior functional mapping/electrophysiological reports (30), indicating that the majority of neurons indeed experienced an intense period of input activity, presumably emanating from layer 4 neurons.

Taken together, our work demonstrates that a SARE reporter, both in vitro and in vivo, can readily trace and mark an ensemble of cells that have experienced intense activity in the recent past. Further works are ongoing to design novel pharmacogenetical and

optogenetical experiments using SARE as a driver for conditional Cre recombinase such as hormone-activated CreER^{T2} (31), or for channelrhodopsins/halorhodopsins (32), with a view to manipulating specific gene expression or neuronal excitability in an activated ensemble of neurons within a circuit.

Materials and Methods

Plasmids, Lentiviruses, and Reagents. Reporter plasmid construction, lentiviral vector preparation, and reagents are described in *SI Materials and Methods*.

Neuronal Culture Preparation, Luciferase Reporter Assay, Fluorescent Protein Reporter Assay, and Luciferase Live-Cell Imaging. Dissociated neuronal culture was prepared from rat embryonic neocortex or postnatal hippocampus as described previously (10, 33). For luciferase assay, cortical neurons were transfected with a firefly luciferase reporter plasmid and an internal control Renilla luciferase plasmid by electroporation. At 10 days in vitro (div), the cells were silenced with TTX for 12–24 h, stimulated with a 4-aminopyridine/bicuculline (4AP/BIC) mixture for 4 h, and lysed. Luciferase activities were measured using the Dual Luciferase assay system (Promega).

For lentiviral reporter assay, hippocampal neurons cultured on coverslips were infected with lentiviruses at 2 div. At 15 div, neurons were silenced with TTX and then stimulated with BDNF (a gift from Dainippon Sumitomo Pharma, Osaka, Japan). For luciferase live-cell imaging, hippocampal neurons transfected with the Arc7000-ELuc-PEST plasmid were imaged in a culture medium containing d-luciferin (0.5 mM, Toyobo) at 14–18 div.

All animal experiments were carried out in accordance with regulations and guidelines of the University of Tokyo and approved by the institutional review committee of University of Tokyo Graduate School of Medicine. More information is provided in *SI Materials and Methods*.

Electrophoretic Mobility Shift Assay (EMSA) and Chromatin Immunoprecipitation (ChIP) Assay. Preparation of brain nuclear extracts is described in *SI Materials and Methods*. The nuclear extracts (2 μg for CREB and SRF and 10 μg for MEF2) were reacted with ^{32}P-radiolabeled DNA probes. Excess amounts (300-fold) of unlabeled probes were added to the reaction mixture for competition assay. Protein-DNA complexes were separated on acrylamide gels and analyzed by an image analyzer (BAS2500, Fujifilm).

Chromatin immunoprecipitation was performed using a kit (Active Motif) essentially following the manufacture's instructions. Precipitates were analyzed using a real-time PCR system (Roche) and gel electrophoresis. More information is provided in *SI Materials and Methods*.

Viral Reporter Assay in Mouse Visual Cortex. Production of lentivirus-infected mice is described in *SI Materials and Methods*. After 3–4 postnatal weeks, the infected mice were subjected to monocular deprivation, dark reared for 1–3 days, exposed to a bright environment for 2–3 h, and then perfused for immunohistochemical analysis. For quantification, infected neurons were identified by native RFP signals and TSA-enhanced GFP-immunoreactive cells were counted. More information is provided in *SI Materials and Methods*.

Statistical Analysis. Statistical analyses were performed using Prism 4.0 (Graphpad Software). Student's paired *t* test and 1-way analysis of variance with repeated measures (ANOVA) followed by Tukey's post hoc test were used for comparisons between 2 groups and 3 groups, respectively. Mann-Whitney *U* test was used for fluorescence reporter assay. All data are shown as mean ± standard error of the mean (SEM), unless otherwise stated.

ACKNOWLEDGMENTS. We thank H. Miyoshi and D. Trono for the lentiviral vector and packaging constructs, respectively; Dainippon Sumitomo Pharma (Osaka, Japan) for supply of BDNF through the courtesy of C. Nakayama and T. Ishiyama; C. Tohyama, M. Kakeyama, and W. Yoshioka (University of Tokyo) for technical help in qPCR analyses; T. Furukawa (Olympus-Japan) for assistance in building a live luciferase imaging microscope. We also thank all members of the Bito laboratory for support and discussion. We are particularly indebted to K. Saiki, Y. Kondo, and T. Kinbara for assistance. This work was supported in part by grants-in-aid from the Ministry of Education, Culture, Sports, Science and Technology (to H.O., M.O., S.T.-K., and H.B.) and from the Ministry of Health, Labor and Welfare (to H.O. and H.B.), by 21st century Center of excellence (COE) and Global COE programs (to H.B.), by a grant from National Institute of Mental Health (MH053608 to P.F.W.), and by awards from the Human Frontier Science Program Organization (career development award to H.O. and a program grant to H.B.), from the Takeda Foundation, from the Toray Science Foundation, and from the Yamada Science Foundation (to H.B.).

1. Kandel ER (2001) The molecular biology of memory storage: a dialogue between genes and synapses. *Science* 294:1030–1038.
2. Bourtchuladze R, *et al.* (1994) Deficient long-term memory in mice with a targeted mutation of the cAMP-responsive element-binding protein. *Cell* 79:59–68.
3. Ramanan N, *et al.* (2005) SRF mediates activity-induced gene expression and synaptic plasticity but not neuronal viability. *Nat Neurosci* 8:759–767.
4. Tokuyama W, Okuno H, Hashimoto T, Xin Li Y, Miyashita Y (2000) BDNF upregulation during declarative memory formation in monkey inferior temporal cortex. *Nat Neurosci* 3:1134–1142.
5. Morris RG (2006) Elements of a neurobiological theory of hippocampal function: the role of synaptic plasticity, synaptic tagging and schemas. *Eur J Neurosci* 23:2829–2846.
6. Pham TA, Impey S, Storm DR, Stryker MP (1999) CRE-mediated gene transcription in neocortical neuronal plasticity during the developmental critical period. *Neuron* 22:63–72.
7. Bliss TV, Collingridge GL (1993) A synaptic model of memory: long-term potentiation in the hippocampus. *Nature* 361:31–39.
8. Bito H, Deisseroth K, Tsien RW (1997) Ca^{2+}-dependent regulation in neuronal gene expression. *Curr Opin Neurobiol* 7:419–429.
9. West AE, Griffith EC, Greenberg ME (2002) Regulation of transcription factors by neuronal activity. *Nat Rev Neurosci* 3:921–931.
10. Bito H, Deisseroth K, Tsien RW (1996) CREB phosphorylation and dephosphorylation: a Ca(2+)- and stimulus duration-dependent switch for hippocampal gene expression. *Cell* 87:1203–1214.
11. Robertson LM, *et al.* (1995) Regulation of c-fos expression in transgenic mice requires multiple interdependent transcription control elements. *Neuron* 14:241–252.
12. Flavell SW, Greenberg ME (2008) Signaling mechanisms linking neuronal activity to gene expression and plasticity of the nervous system. *Annu Rev Neurosci* 31:563–590.
13. Link W, *et al.* (1995) Somatodendritic expression of an immediate early gene is regulated by synaptic activity. *Proc Natl Acad Sci USA* 92:5734–5738.
14. Lyford GL, *et al.* (1995) Arc, a growth factor and activity-regulated gene, encodes a novel cytoskeleton-associated protein that is enriched in neuronal dendrites. *Neuron* 14:433–445.
15. Plath N, *et al.* (2006) Arc/Arg3.1 is essential for the consolidation of synaptic plasticity and memories. *Neuron* 52:437–444.
16. Shepherd JD, *et al.* (2006) Arc/Arg3.1 mediates homeostatic synaptic scaling of AMPA receptors. *Neuron* 52:475–484.
17. Chowdhury S, *et al.* (2006) Arc/Arg3.1 interacts with the endocytic machinery to regulate AMPA receptor trafficking. *Neuron* 52:445–459.
18. Guzowski JF, *et al.* (2000) Inhibition of activity-dependent arc protein expression in the rat hippocampus impairs the maintenance of long-term potentiation and the consolidation of long-term memory. *J Neurosci* 20:3993–4001.
19. Guzowski JF, McNaughton BL, Barnes CA, Worley PF (1999) Environment-specific expression of the immediate-early gene Arc in hippocampal neuronal ensembles. *Nat Neurosci* 2:1120–1124.
20. Han JH, *et al.* (2007) Neuronal competition and selection during memory formation. *Science* 316:457–460.
21. Tagawa Y, Kanold PO, Majdan M, Shatz CJ (2005) Multiple periods of functional ocular dominance plasticity in mouse visual cortex. *Nat Neurosci* 8:380–388.
22. Ramirez-Amaya V, *et al.* (2005) Spatial exploration-induced Arc mRNA and protein expression: evidence for selective, network-specific reactivation. *J Neurosci* 25:1761–1768.
23. Waltereit R, *et al.* (2001) Arg3.1/Arc mRNA induction by Ca^{2+} and cAMP requires protein kinase A and mitogen-activated protein kinase/extracellular regulated kinase activation. *J Neurosci* 21:5484–5493.
24. Li L, Carter J, Gao X, Whitehead J, Tourtellotte WG (2005) The neuroplasticity-associated arc gene is a direct transcriptional target of early growth response (Egr) transcription factors. *Mol Cell Biol* 25:10286–10300.
25. Wallace CS, Lyford GL, Worley PF, Steward O (1998) Differential intracellular sorting of immediate early gene mRNAs depends on signals in the mRNA sequence. *J Neurosci* 18:26–35.
26. Thomas GM, Huganir RL (2004) MAPK cascade signalling and synaptic plasticity. *Nat Rev Neurosci* 5:173–183.
27. Hashimoto M, Mikoshiba K (2004) Neuronal birthdate-specific gene transfer with adenoviral vectors. *J Neurosci* 24:286–296.
28. Flavell SW, *et al.* (2006) Activity-dependent regulation of MEF2 transcription factors suppresses excitatory synapse number. *Science* 311:1008–1012.
29. Davis FJ, Gupta M, Camoretti-Mercado B, Schwartz RJ, Gupta MP (2003) Calcium/calmodulin-dependent protein kinase activates serum response factor transcription activity by its dissociation from histone deacetylase, HDAC4. Implications in cardiac muscle gene regulation during hypertrophy. *J Biol Chem* 278:20047–20058.
30. Bear MF, Kleinschmidt A, Gu QA, Singer W (1990) Disruption of experience-dependent synaptic modifications in striate cortex by infusion of an NMDA receptor antagonist. *J Neurosci* 10:909–925.
31. Feil R, Wagner J, Metzger D, Chambon P (1997) Regulation of Cre recombinase activity by mutated estrogen receptor ligand-binding domains. *Biochem Biophys Res Commun* 237:752–757.
32. Zhang F, Aravanis AM, Adamantidis A, de Lecea L, Deisseroth K (2007) Circuit-breakers: optical technologies for probing neural signals and systems. *Nat Rev Neurosci* 8:577–581.
33. Takemoto-Kimura S, *et al.* (2007) Regulation of dendritogenesis via a lipid-raft-associated Ca^{2+}/calmodulin-dependent protein kinase CLICK-III/CaMKIgamma. *Neuron* 54:755–770.

NEUROSCIENCE

frontiers in
BEHAVIORAL NEUROSCIENCE

ORIGINAL RESEARCH ARTICLE
published: 14 August 2009
doi: 10.3389/neuro.08.012.2009

Litter environment affects behavior and brain metabolic activity of adult knockout mice

***David Crews*[1]*, *David Rushworth*[1], *Francisco Gonzalez-Lima*[2] *and Sonoko Ogawa*[3]**

[1] *Section of Integrative Biology, University of Texas at Austin, Austin, TX, USA*
[2] *Institute of Neuroscience and the Department of Psychology, University of Texas at Austin, Austin, TX, USA*
[3] *Laboratory of Behavioral Neuroendocrinology, Graduate School of Comprehensive Human Sciences, University of Tsukuba, Ibaraki, Japan*

Edited by:
Larry J. Young, Emory University, USA; Yerkes National Primate Research Center, USA

Reviewed by:
Lance Kriegsfeld, University of California, USA
Emily Rissman, University of Virginia, USA

***Correspondence:**
David Crews, Section of Integrative Biology, University of Texas at Austin, Austin, TX 78712, USA.
e-mail: crews@mail.utexas.edu

In mammals, the formative environment for social and anxiety-related behaviors is the family unit; in the case of rodents, this is the litter and the mother-young bond. A deciding factor in this environment is the sex ratio of the litter and, in the case of mice lacking functional copies of gene(s), the ratio of the various genotypes in the litter. Both Sex and Genotype ratios of the litter affect the nature and quality of the individual's behavior later in adulthood, as well as metabolic activity in brain nuclei that underlie these behaviors. Mice were raised in litters reconstituted shortly after to birth to control for sex ratio and genotype ratio (wild type pups versus pups lacking a functional estrogen receptor α). In both males and females, the Sex and Genotype of siblings in the litter affected aggressive behaviors as well as patterns of metabolic activity in limbic nuclei in the social behavior network later in adulthood. Further, this pattern in males varied depending upon the Genotype of their brothers and sisters. Principal Components Analysis revealed two components comprised of several amygdalar and hypothalamic nuclei; the VMH showed strong correlations in both clusters, suggesting its pivotal nature in the organization of two neural networks.

Keywords: life history, sex differences, genotype differences, sibling, aggression

INTRODUCTION

Adult sociosexual behavior is the cumulative result of genetics and experience. These experiences begin prenatally in the intrauterine environment, and continue in early postnatal life according to litter composition and maternal behavior, influencing how the individual interacts with the social environment in adulthood (Crews, 1999; Crews and Groothuis, 2005; Fleming et al., 2002; Meaney, 2001; Moore, 1995; Moore et al., 1997; Sakata et al., 2001). Various studies indicate that experiences can be imprinted epigenetically to influence future generations (Bateson, 2005; Crews, 2008; Crews et al., 2007; Crews and McLachlan, 2006; Gottlieb, 2002; Jablonka and Lamb, 1995; Lewontin, 2000; Waddington, 1942, 1953; West-Eberhard, 2003).

Complex behaviors such as aggressive, affiliative behaviors, and anxiety-related behaviors depend upon concerted interaction of many brain nuclei acting together, not in isolation. Extensive research has revealed that specific nuclei involved in the regulation of behavior are reciprocally interconnected, often express receptors for steroid hormones, and function in concert as a neural network. Newman (1999) proposed that behavioral traits depend ultimately upon this social behavior network. Behavioral traits depend ultimately upon the ability of this network(s) of nuclei and neurons to sustain a certain level of metabolic activity necessary for interaction. Of particular interest is how these nuclei might be functionally associated in the adult, and how early environment might change these functional associations. A method that enables study of the long-term consequences of life history changes is cytochrome oxidase IV (COX) quantitative enzyme histochemistry (Sakata et al., 2005). COX, complex IV of the mitochondrial respiratory chain, the rate-limiting enzyme for the production of utilizable energy derived by coupling oxidative metabolism to the production of ATP. Thus, the abundance of COX serves as an endogenous marker of metabolic capacity in nuclei and neurons, portraying the result of long-term metabolic demand as well as the capacity of a network of nuclei to support specific behaviors. Previous work with rodents reveals that early experience (both pre- and postnatal) significantly affects COX activity in the adult limbic forebrain nuclei and that early experience can modify functional associations of nuclei within integrated neural circuits (c.f., Crews et al., 2006; Jones et al., 1997; Sakata et al., 2002).

In behavioral research with rodents in general, and genetically modified mice in particular, the sex and/or genotype ratios of the

Abbreviations: ♀WT, female wildtype mouse; ♀KO, female estrogen receptor α knockout mouse; ♂WT, male wildtype mouse; ♂KO, male estrogen receptor α knockout mouse; ACo, anterior cortical amygdaloid nucleus; AHA, anterior hypothalamic area, anterior; AVPe, anteroventral periventricular nucleus (=AVPV); BST, bed nucleus of the stria terminalis, including anterior and lateral ventral divisions; BSTMA, bed nucleus of the stria terminalis medial division, anterior; BSTMPM, bed nucleus of the stria terminalis, medial division, posteromedial; CeA, central amygdaloid nucleus; CLC, caudal limbic cluster; cMPOA, caudal medial preoptic area; CO, cytochrome c oxidase, complex IV, EC 1.9.3.1; ERα, estrogen receptor α; KO, ERα knockout; LHb, lateral habenular nucleus; LSI, lateral septal nucleus intermediate; MeAA, medial amygdaloid (MeA) nucleus, anterior; MeAPD, medial amygdaloid (MeA) nucleus, posterodorsal; MeAPV, medial amygdaloid (MeA) nucleus, posteroventral; MHb, medial habenular nucleus; MPOA, medial preoptic area; PaN, paraventricular hypothalamic nucleus; PC, principal component; Pe, periventricular hypothalamic nucleus; RLC, rostral limbic cluster; rMPOA, rostral medial preoptic area; VMH, ventromedial hypothalamic nucleus, including rostral and central VMH; VMHDM, ventromedial hypothalamic nucleus, dorsomedial; VMHVL, ventromedial hypothalamic nucleus, ventrolateral.